Supplementary Material:

A comparative study of the oxidation of toluene and the three isomers of xylene

Ismahane Meziane, Nicolas Delort, Olivier Herbinet, Roda Bounaceur,

Frédérique Battin-Leclerc

Université de Lorraine, CNRS, LRGP, F-54000 Nancy, France

Outline

1/ GC analysis of the initial fuel

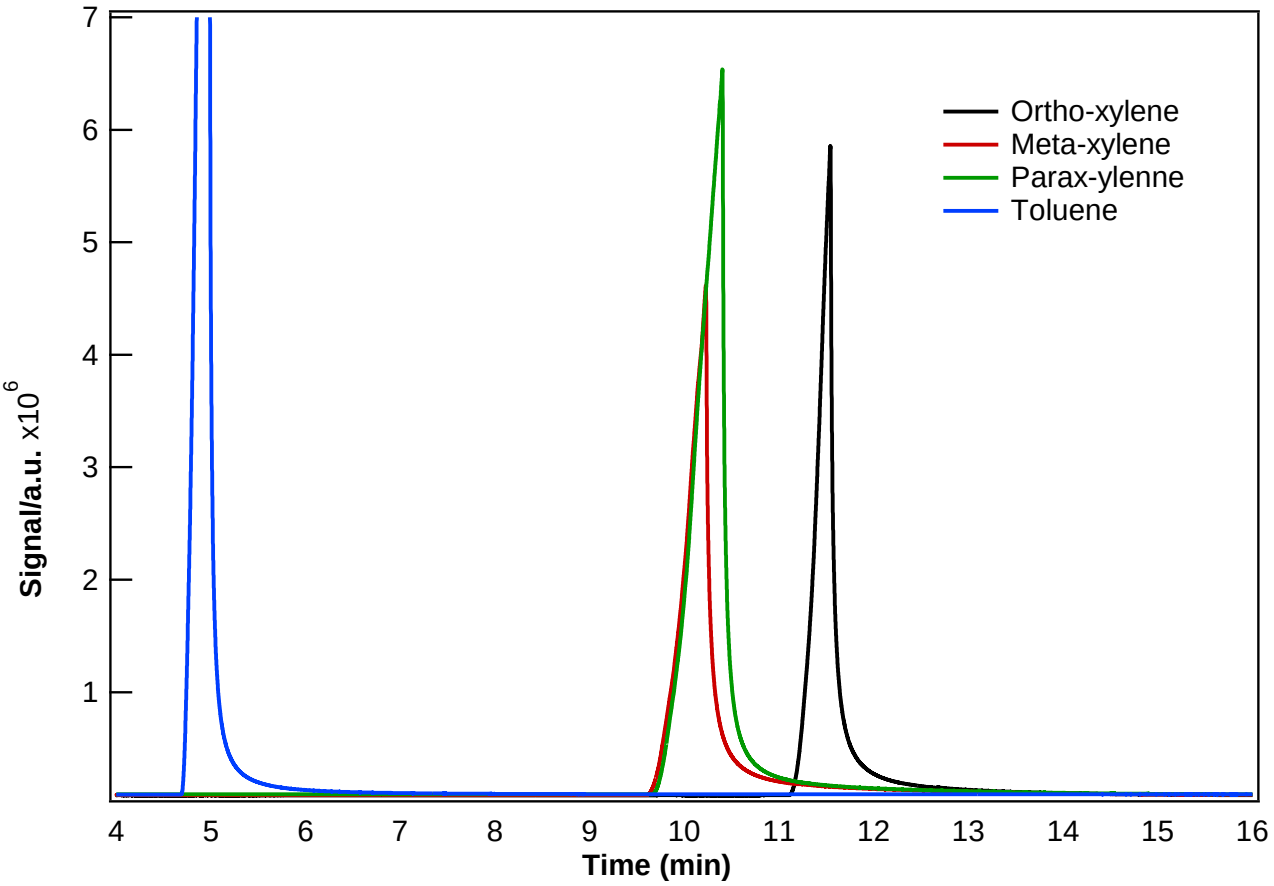

Figure S1: Chromatogram of the four unreacted fuels obtained using the GC equipped with the HP-5 capillary column.

2/ List of detected products and material balance

Table S1: Detected products according to the fuel (***Plot Q column)***.

Retention time	Chemical name	Structure	Toluene	o-Xylene	m-Xylene	p-Xylene
3.1	Carbon monoxide	CO	Q	Q	Q	Q
3.8	Carbon dioxide	CO_2	Q	Q	Q	Q
4.7	Ethylene	C_2H_4	Q	Q	Q	Q
5.0	Acetylene	C_2H_2	Q	Q	D	Q
5.5	Ethane	C_2H_6	Q	Q	Q	Q
14.1	Propene	C_3H_6	Q	Q	Q	Q
16.2	Allene	a-C_3H_4	D	D	D	D
17.1	Propyne	p-C_3H_4	D	D	D	D
22	Acetaldehyde	CH_3CHO	Q	Q	Q	Q
24.6	1-Butene	C_4H_8	D	D	D	D
25	1,3-Butadiene	C_4H_6	Q	Q	Q	D
29	Furan	C_4H_4O	D	Q	D	Q
29.5	Acrolein	CH_2CHCHO	Q	Q	Q	D
30.7	Acetone	CH_3COCH_3	D	Q	D	D
31.9	1,3-Cyclopentadiene	C_5H_6	D	Q	Q	Q
32.2	1,3-Pentadiene	C_5H_8	D	D	D	D
34.7	Methacrolein	$CH_2(CH_3)CCHO$	D	D	D	D

D: Detected; Q: Quantified; R: Reactant.

Table S2: Detected products according to the fuel (***HP 5 column)***, with their boiling point ($T_{boil.}$) and melting point ($T_{melt.}$(in red, those above 300K)) at atmospheric pressure.

Retention time	Chemical name	Structure	($T_{boil.}$-$T_{melt.}$) (K)	Toluene	o-Xylene	m-Xylene	p-Xylene
3.7	Cyclopentene	C_5H_8	(317, 138)	D	D	D	D
4.7	1,3-Cyclopentadiene	C_5H_6	(314, 183)	Q	Q	Q	Q
4.9	1,3-Cyclohexadiene	C_6H_8	(354, 184)	D	D	D	D
5	Benzene	C_6H_6	(353, 278)	Q	Q	Q	Q
8	Toluene	C_7H_8	(383, 178)	R	Q	Q	Q
15.7	Ethylbenzene	C_8H_{10}	(409, 179)	Q	Q	Q	Q
16.7	p, m-Xylene	C_8H_{10}	(411, 286) (412, 225)	-	-	R	R
19.4	Styrene	C_8H_8	(419, 240)	Q	D (Co-eluted with o-xylene)	Q	Q
19.9	o-Xylene	C_8H_{10}	(417, 248)	Q	R	-	-
25.3	Phenyl-oxirane	C_8H_8O	(467, 236)	D	D	-	-
25.9	Cumene	C_9H_{12}	(425, 177)	-	D	-	-
32.6	Benzaldehyde	C_7H_6O	(452, 247)	Q	Q	Q	Q
34.9	Ethyl methylbenzene	C_9H_{12}	(437, 256)	Q	Q	Q	Q
36.1	Phenol	C_6H_6O	(455, 314)	Q	Q	-	Q
36.2	Methylstyrene	C_9H_{10}	(439,171)	-	Q	Q	Q
36.3	Benzofuran	C_8H_6O	(446, 255)	Q	Q	Q	Q
36.8	1,3-Benzodioxole	$C_7H_6O_2$	(445, 255)	Q	Q	-	Q
39.6	Indene	C_9H_8	(454, 271)	Q	Q	Q	Q
39.7	o-, m-, p-Hydroxy-benzaldehyde	C_7H_6O	(583,385) (583,385) (583,385)	Q	Q	Q	Q
40.7	o-Cresol	C_7H_8O	(464, 304)	Q	Q	-	-
40.9	o-, m-, p-Methylbenzaldehyde	C_8H_8O	(473, 238) (472, <300) (477, 267)	-	Q	Q	Q
41.6	2,3-Dihydrobenzo-furan	C_8H_8O	(461, 250)	D	D	Q	-
41.7	Phthalan	C_8H_8O	(465, 279)	-	Q	-	-
41.9	m, p-Cresol	C_7H_8O	(475, 284) (476,307)	-	-	Q	-
45.9	Naphthalene	$C_{10}H_8$	(490, 353)	Q	-	-	-
46.1	E-cinnamaldehyde	C_9H_8O	(521, 265)	D	-	-	-
49.5	1-Methylnaphtahlene	$C_{11}H_{10}$	(517, 242)	D	-	-	-
55.4	Stilbene	$C_{14}H_{12}$	(580, 397)	Q	-	-	-

D: Detected; Q: Quantified; R: Reactant.

Table S2: Carbon atom balance during o- and p-xylene oxidation.

	Carbon balance (o-Xylene)			Carbon balance (p-Xylene)		
T(K)	**ϕ =0.5**	**ϕ =1.0**	**ϕ =2.0**	**ϕ =0.5**	**ϕ =1.0**	**ϕ =2.0**
600	98%	106%	102%	93%	101%	107%
625	98%	106%	102%	105%	103%	114%
650	101%	101%	101%	99%	101%	104%
675	102%	101%	101%	99%	102%	103%
700	103%	100%	98%	100%	102%	91%
725	103%	101%	100%	99%	103%	98%
750	102%	96%	101%	102%	104%	97%
775	101%	100%	100%	106%	107%	104%
800	101%	103%	102%	107%	103%	100%
825	99%	102%	101%	101%	102%	97%
850	99%	103%	98%	98%	109%	102%
875	107%	106%	98%	97%	104%	106%
900	84%	106%	100%	96%	111%	103%
925	94%	99%	100%	99%	107%	103%
950	88%	92%	102%	96%	94%	108%
975	92%	96%	88%	104%	102%	101%
1000	108%	89%	91%	100%	81%	87%
1025	122%	89%	88%	106%	81%	89%
1050	106%	101%	80%	106%	75%	90%
1075	102%	106%	91%	105%	84%	104%
1100	102%	82%	89%	106%	95%	100%

Table S3: Carbon atom balance during m-xylene and toluene oxidation.

	Carbon balance (m-Xylene)			Carbon balance (Toluene)		
T(K)	**ϕ=0.5**	**ϕ =1.0**	**ϕ =2.0**	**ϕ =0.5**	**ϕ =1.0**	**ϕ =2.0**
600	102%	104%	100%	–	–	–
625	104%	100%	99%	–	–	–
650	102%	102%	102%	–	–	
675	105%	104%	103%	–	–	–
700	103%	103%	99%	99%	102%	100%
725	99%	98%	106%	101%	101%	102%
750	97%	97%	104%	102%	100%	98%
775	100%	98%	98%	103%	99%	103%
800	100%	103%	98%	99%	106%	108%
825	100%	101%	105%	106%	104%	104%
850	99%	103%	97%	104%	110%	106%
875	95%	103%	100%	104%	105%	108%
900	98%	100%	111%	98%	105%	108%
925	79%	98%	103%	100%	105%	103%
950	86%	85%	111%	90%	101%	108%
975	84%	102%	107%	95%	98%	107%
1000	83%	105%	130%	96%	99%	103%
1025	84%	96%	86%	86%	99%	94%
1050	86%	89%	88%	95%	77%	92%
1075	84%	88%	94%	91%	113%	98%
1100	88%	91%	91%	107%	110%	105%

3/ Validation of the COLIBRI model on main literature data

3.1/ Validation on existing toluene data

- **Species mole fraction in Jet Stirred Reactor**

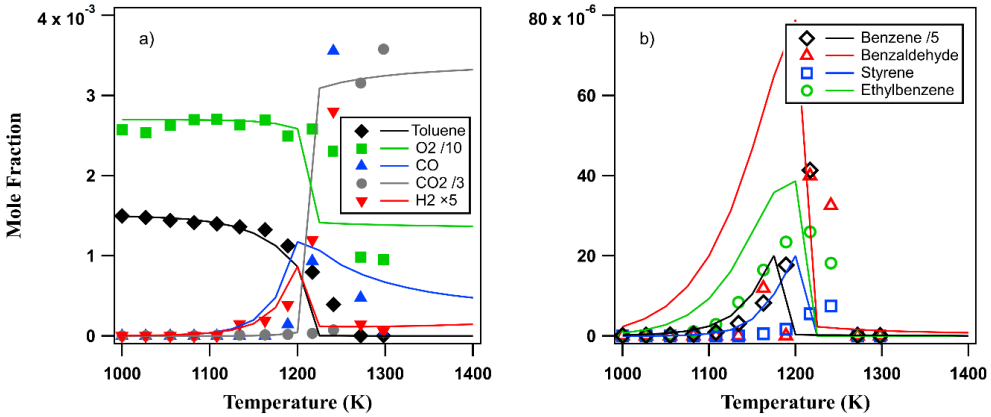

Figure S2: Validation on experimental mole fraction profiles obtained by Dagaut et al. [1] during the oxidation of toluene in JSR at Φ=0.5 (τ=0.07 s, P=1 atm). a) fuel and main light species, b) main aromatic compounds.

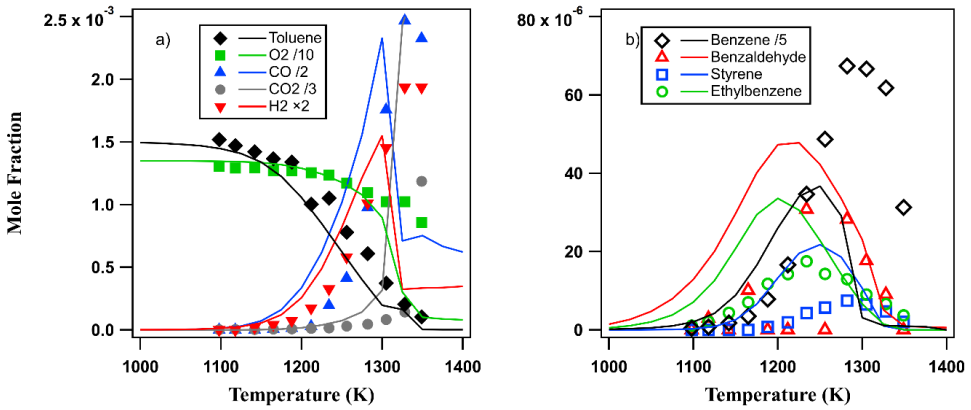

Figure S3: Validation on experimental mole fraction profiles obtained by Dagaut et al. [1] during the oxidation of toluene in JSR at Φ=1 (τ=0.1 s, P=1 atm). a) fuel and main light species, b) main aromatic compounds.

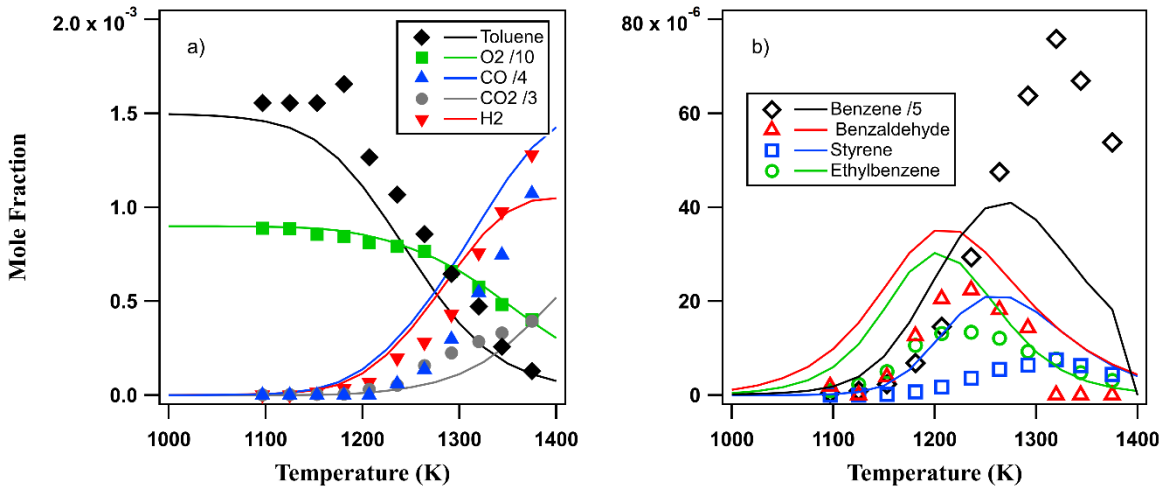

Figure S4: Validation on experimental mole fraction profiles obtained by Dagaut et al. [1] during the oxidation of toluene in JSR at Φ=1.5 (τ=0.12 s, P=1 atm). a) fuel and main light species, b) main aromatic compounds.

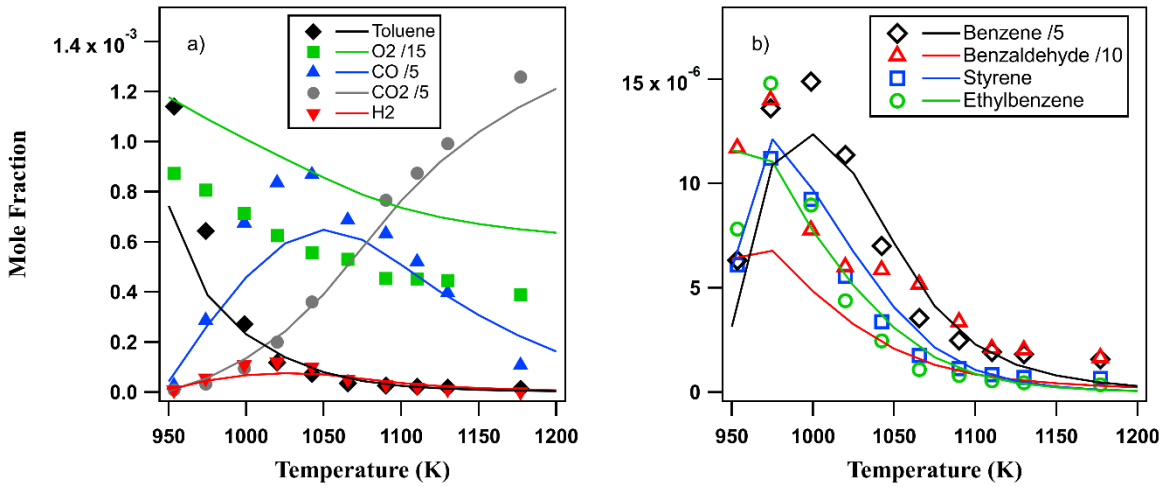

Figure S5: Validation on experimental mole fraction profiles obtained by Yuan et al. [2] during the oxidation of toluene in JSR at Φ=0.5 (τ=0.6 s, P=10 atm). a) fuel and main light species, b) main aromatic compounds.

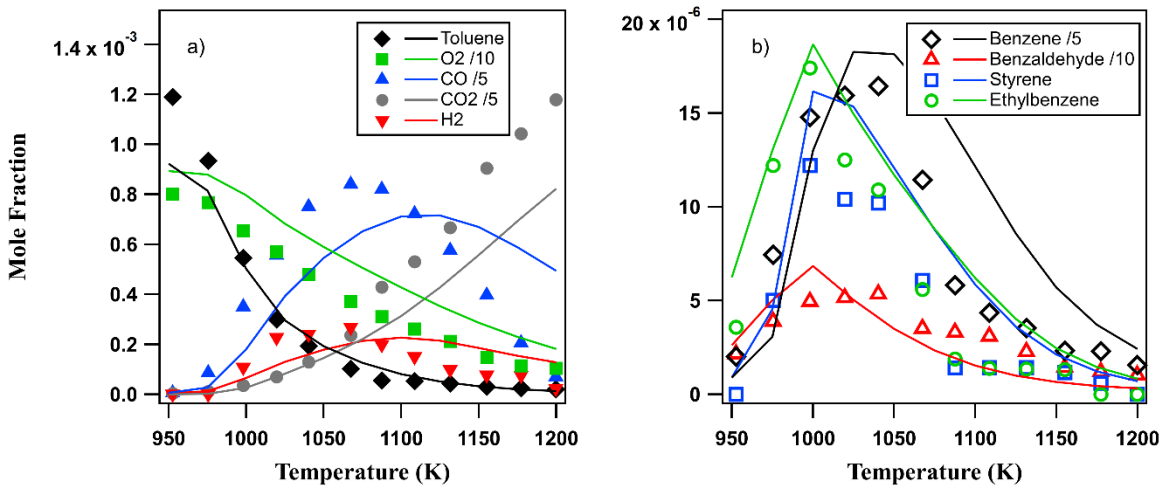

Figure S6: Validation on experimental mole fraction profiles obtained by Yuan et al. [2] during the oxidation of toluene in JSR at Φ=1 (τ=0.6 s, P=10 atm). a) fuel and main light species, b) main aromatic compounds.

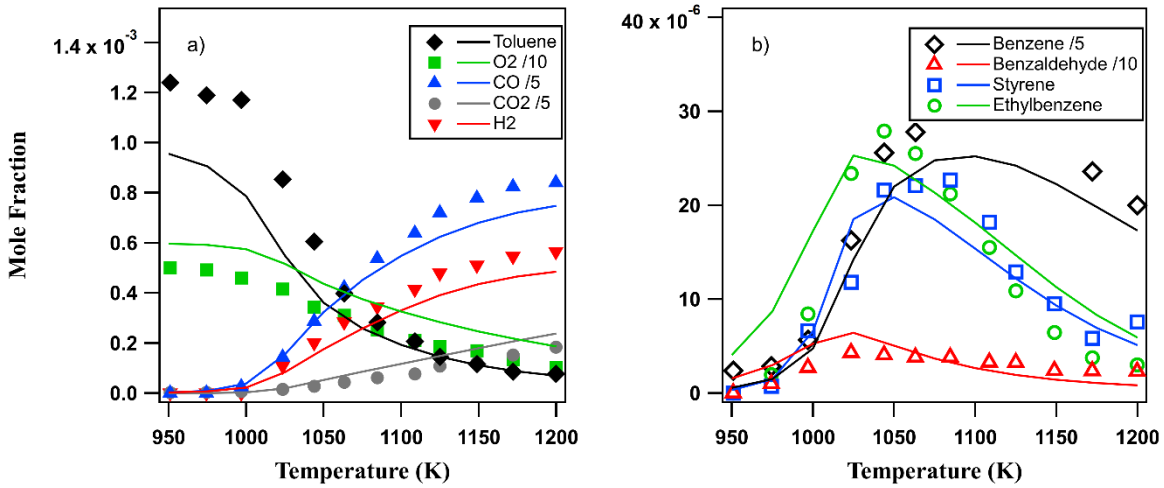

Figure S7: Validation on experimental mole fraction profiles obtained by Yuan [2] et al. during the oxidation of toluene in JSR at Φ=1.5 (τ=0.6 s, P=10 atm). a) fuel and main light species, b) main aromatic compounds.

- **Ignition delay times**

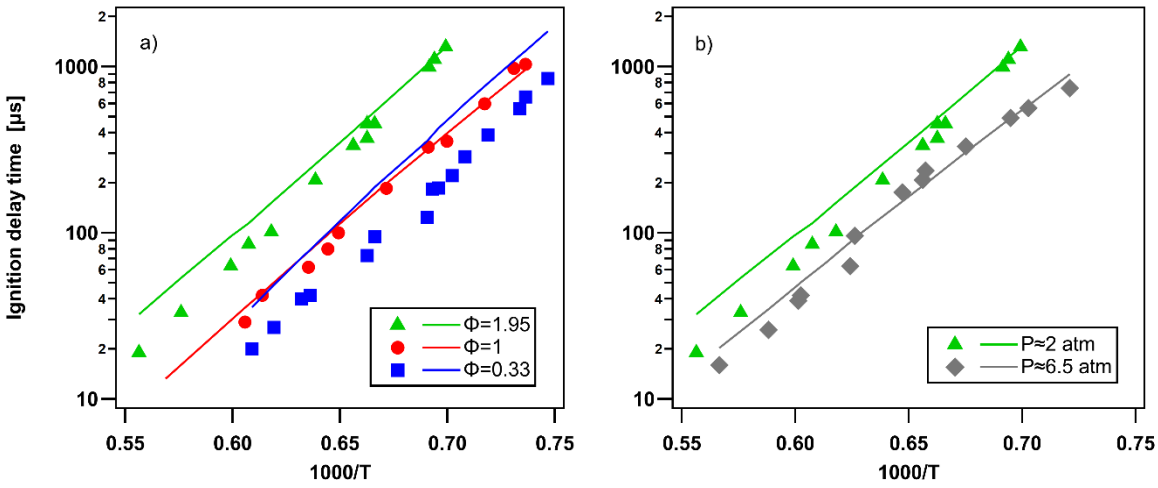

Figure S8: Validation on ignition delay time measurements obtained by Burcat et al. [3] in shock tube for a) post shock pressures around 2 atm, b) Φ=1.95.

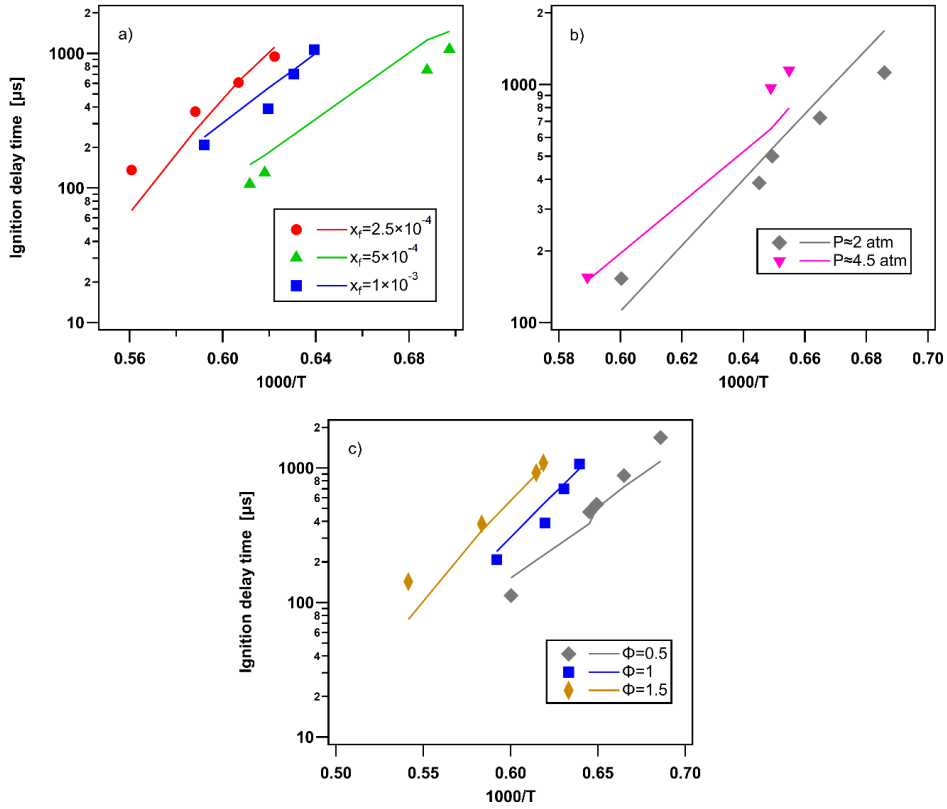

Figure S9: Validation on ignition delay time measurements obtained by Vasudevan et al. [4] in shock tube for a) Φ=1 and $P_{post\ shock} \approx 2$ atm, b) Φ=0.5 and $x_{fuel}=10^{-3}$, c) $P_{post\ shock} \approx 2$ atm and $x_{fuel}=10^{-3}$.

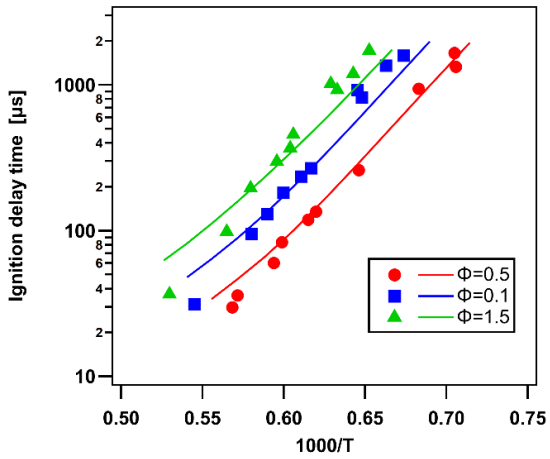

Figure S10: Validation on ignition delay time measurements obtained by Pengloan et al. [5] in a shock tube for post shock pressure around 1.1 atm.

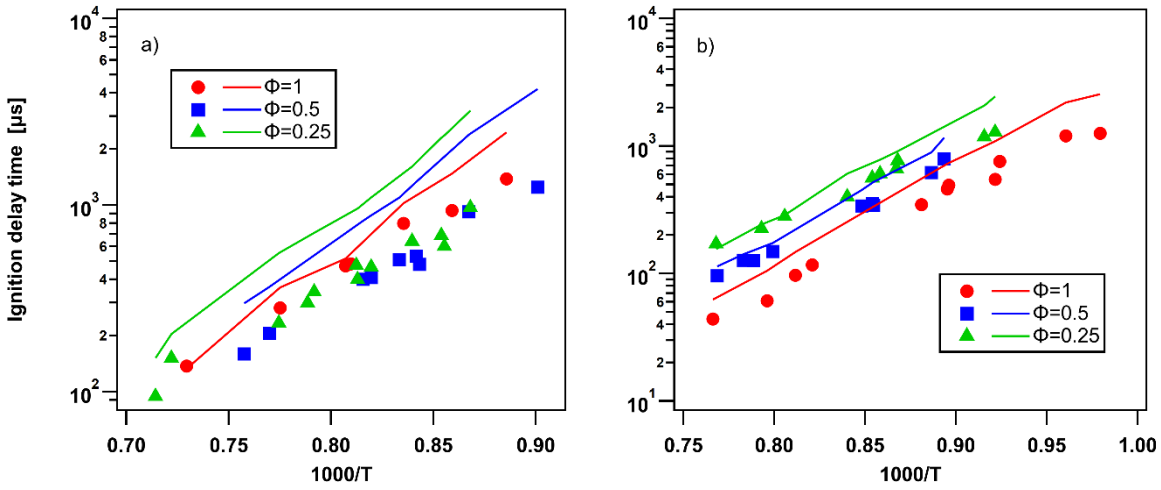

Figure S11: Validation on ignition delay time measurements obtained by Shen et al. [6] in shock tube for post shock pressure around a) 12 atm, b) 50 atm.

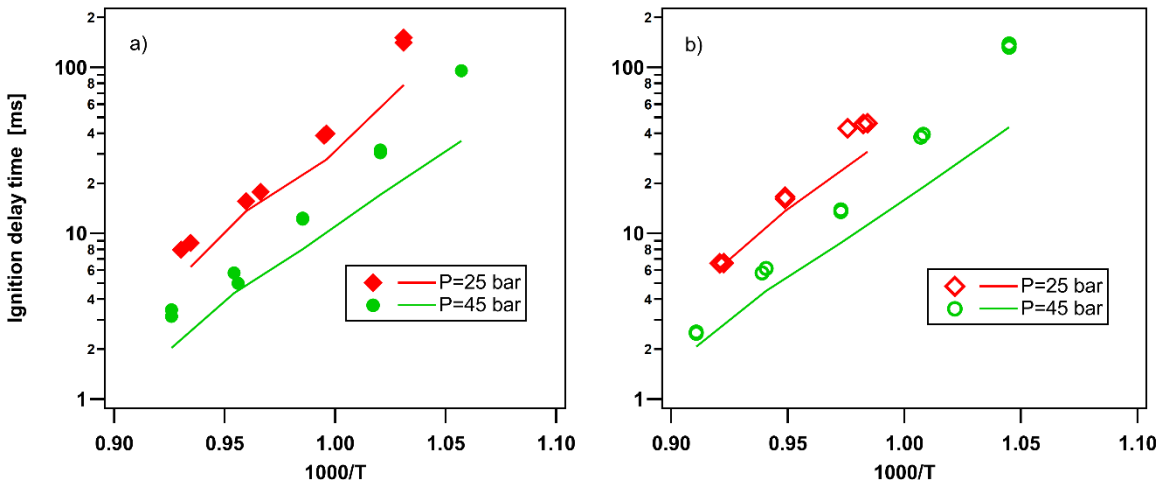

Figure S12: Validation on ignition delay time measurements obtained by Kukkadapu et al. [7] in a rapid compression machine for equivalence ratios of a) Φ=1, b) Φ=0.5.

- **Mole fraction profiles in shock tube**

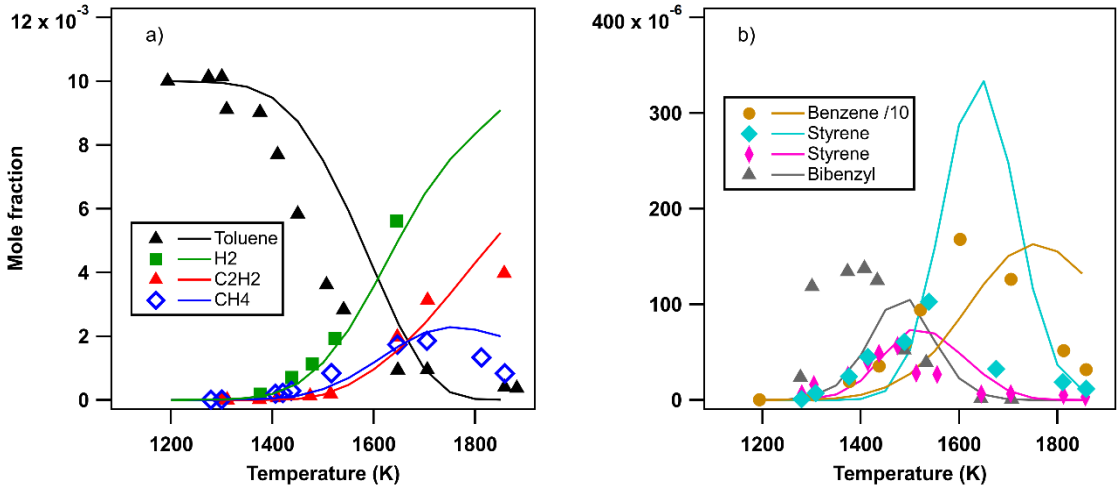

Figure S13: Validation on mole fraction profiles obtained by Colket et al. [8] during the pyrolysis of toluene in a shock tube for post shock pressure around 10 atm and τ=600 µs. a) fuel and main light species, b) main aromatic compounds.

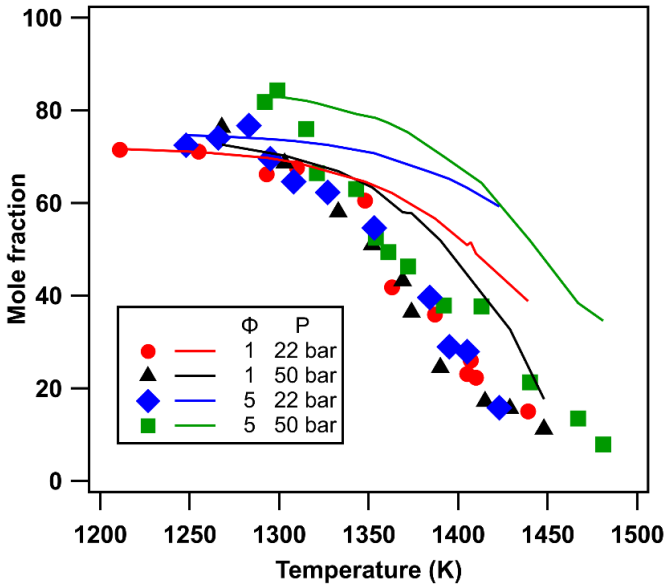

Figure S14: Validation on toluene mole fraction profile during oxidation of toluene in shock tube by Sivaramakrishnan et al. [9].

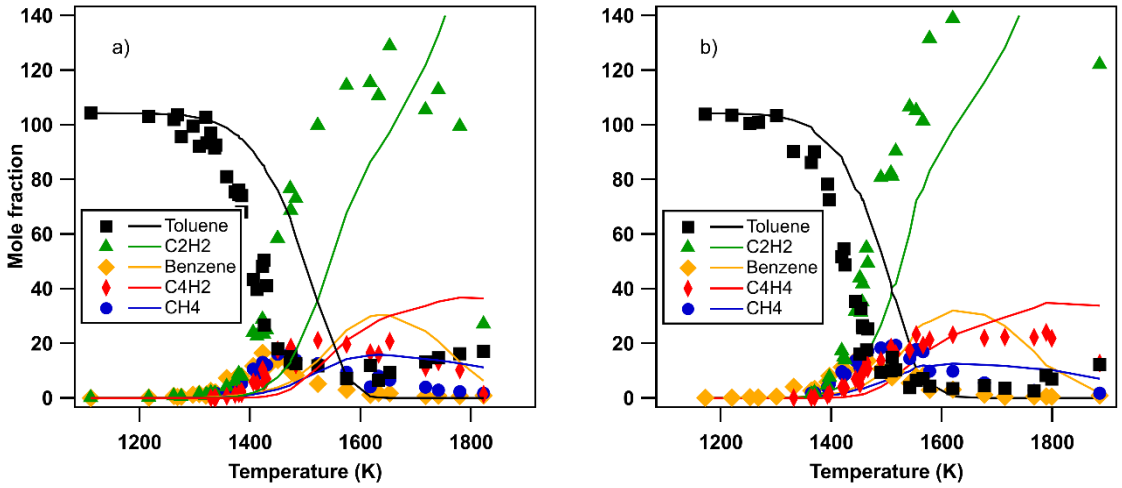

Figure S15: Validation on main species mole fraction profile during the pyrolysis of toluene in shock tube by Sivaramakrishnan et al. [10] for post shock pressure around a) 27 atm, b) 45 atm.

- **Plug Flow Reactor**

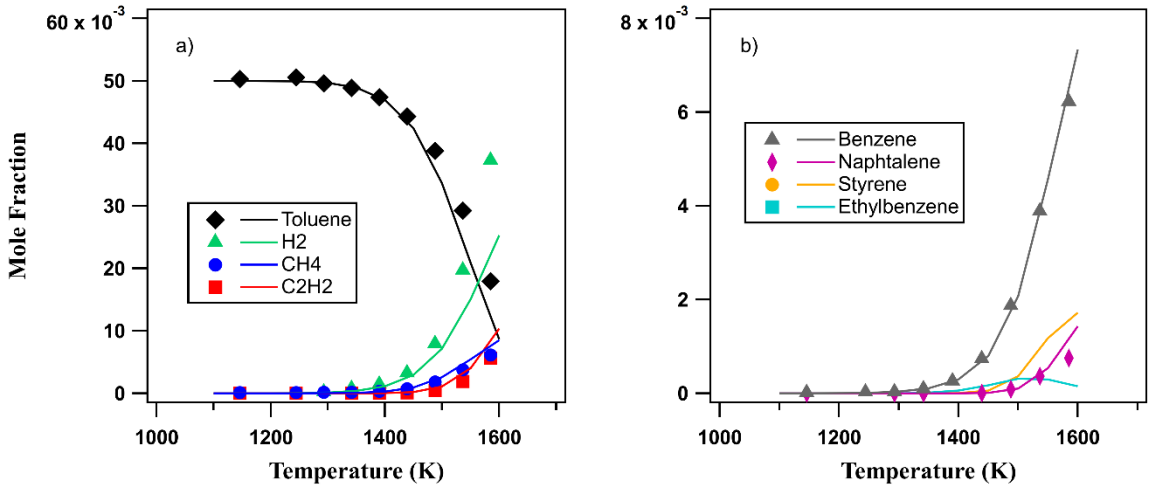

Figure S16: Validation on mole fraction profiles obtained by Yuan et al. [2] during the pyrolysis of toluene in a plug flow reactor under 4.10^{-2} atm, a) fuel and main light species, b) main aromatic compounds.

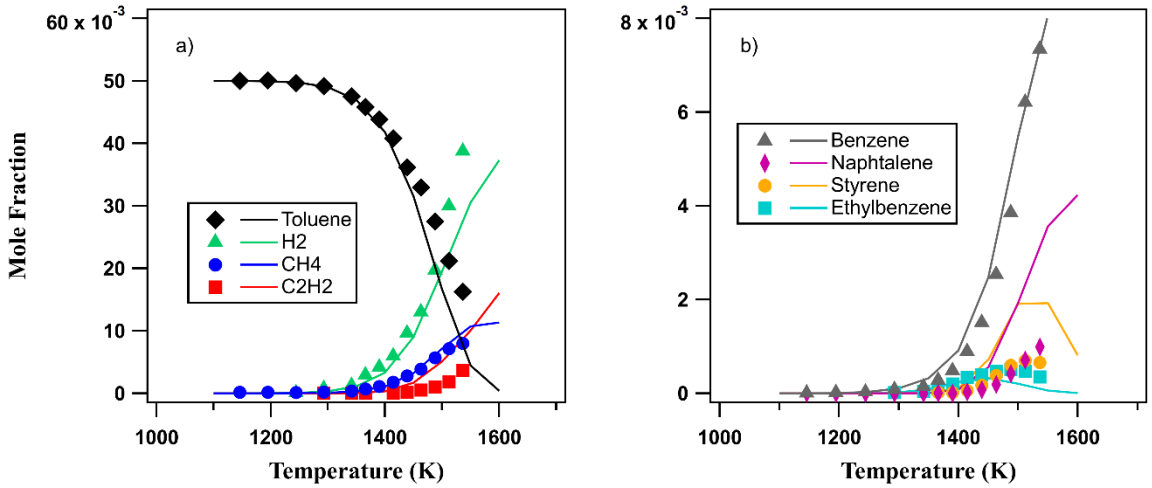

Figure S17: Validation on mole fraction profiles obtained by Yuan et al. [2] during the pyrolysis of toluene in a plug flow reactor under $1{,}067.10^{-1}$ atm , a) fuel and main light species, b) main aromatic compounds.

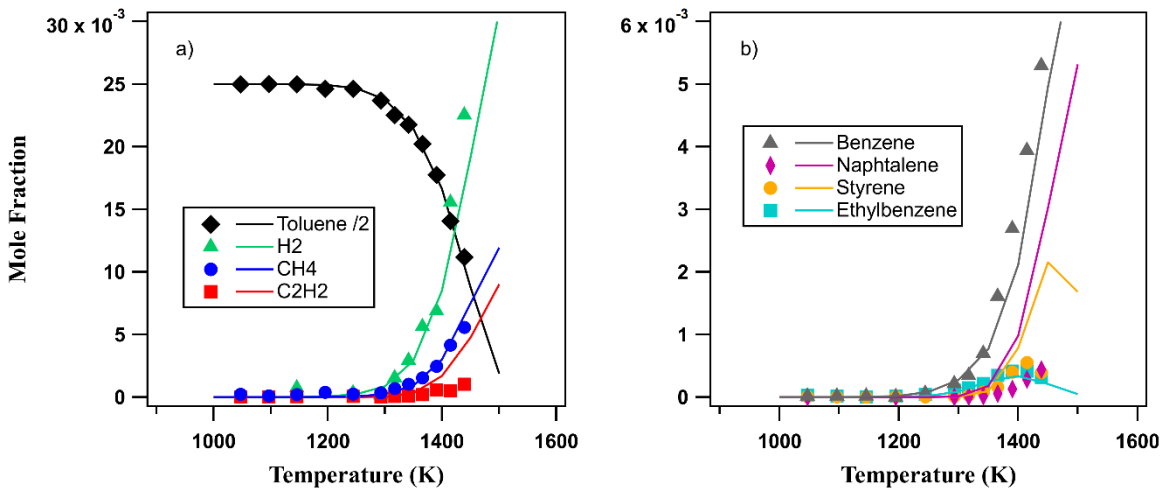

Figure S18: Validation on mole fraction profiles obtained by Yuan et al. [2] during the pyrolysis of toluene in a plug flow reactor under 2,666.10^{-1} atm , a) fuel and main light species, b) main aromatic compounds.

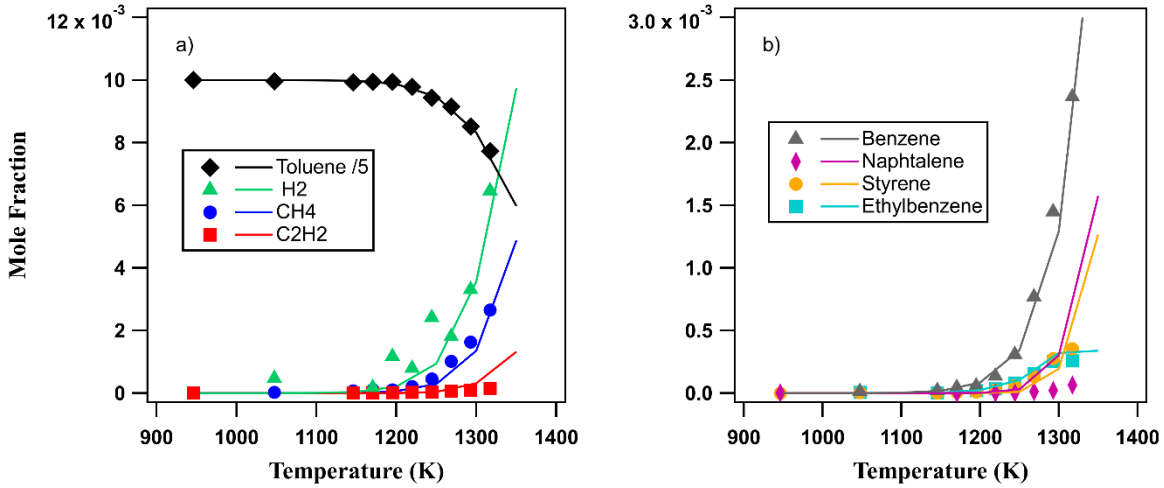

Figure S19: Validation on mole fraction profiles obtained by Yuan et al. [2] during the pyrolysis of toluene in a plug flow reactor under 1 atm , a) fuel and main light species, b) main aromatic compounds.

- **Flame structure**

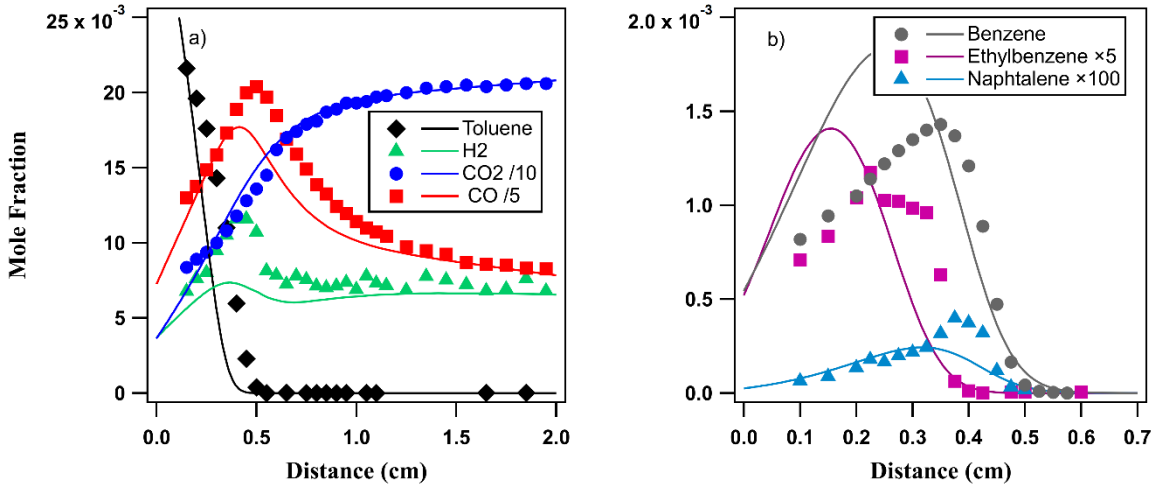

Figure S20: Validation on mole fraction profiles obtained by Li et al. [11] in a toluene-O_2-Ar flame at Φ=0.75 under 4.10^{-2} bar, a) fuel and main light species, b) main aromatic compounds.

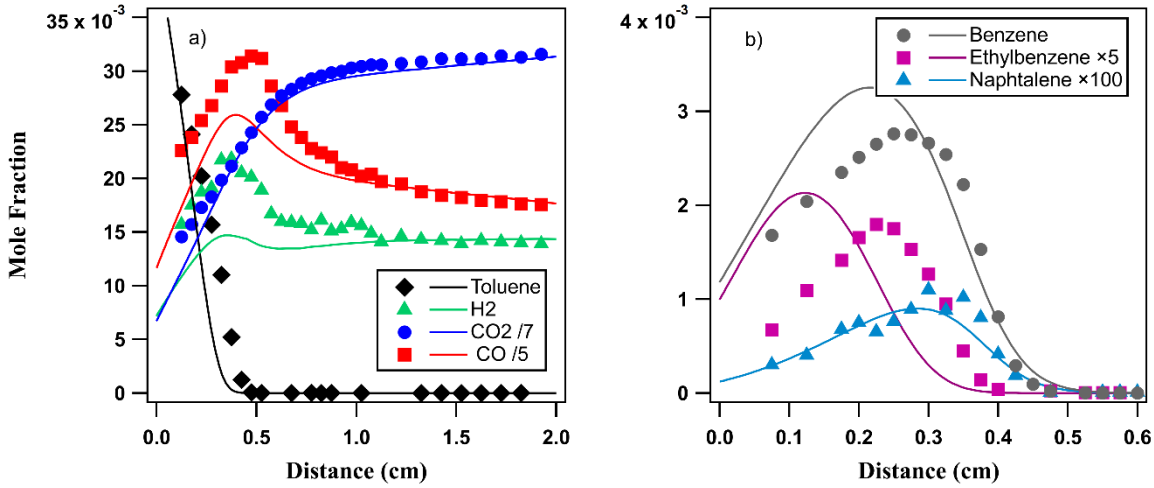

Figure S21: Validation on mole fraction profiles obtained by Li et al. [11] in a toluene-O_2-Ar flame at Φ=1 under 4.10^{-2} bar, a) fuel and main light species, b) main aromatic compounds.

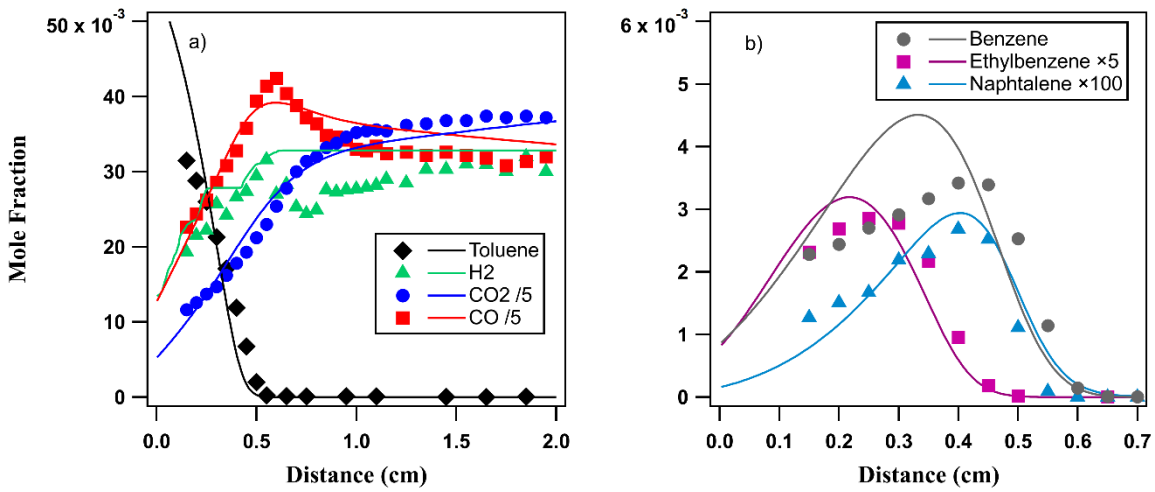

Figure S22: Validation on mole fraction profiles obtained by Li et al. [11] in a toluene-O_2-Ar flame at Φ=1.25 under 4.10^{-2} bar, a) fuel and main light species, b) main aromatic compounds.

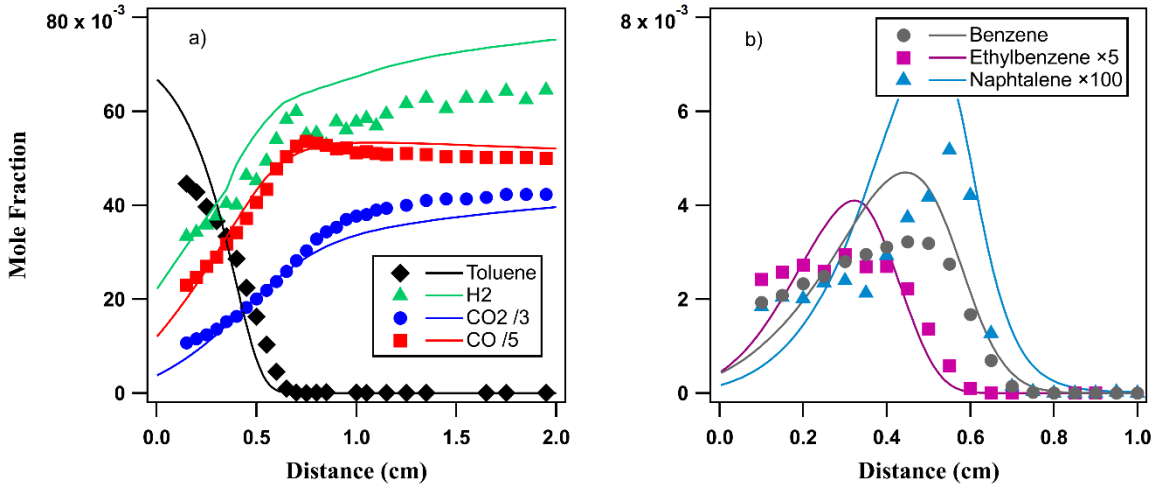

Figure S23: Validation on mole fraction profiles obtained by Li et al. [11] in a toluene-O_2-Ar flame at Φ=1.5 under 4.10^{-2} bar, a) fuel and main light species, b) main aromatic compounds.

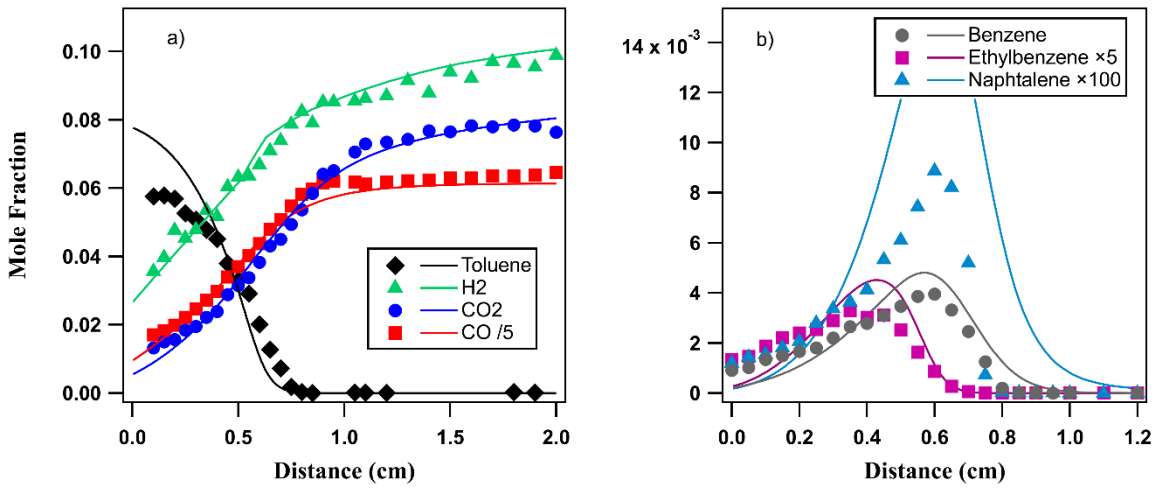

Figure S24: Validation on mole fraction profiles obtained by Li et al. [11] in a toluene-O_2-Ar flame at Φ=1.75 under 4.10^{-2} bar, a) fuel and main light species, b) main aromatic compounds.

- **Laminar Burning Velocities**

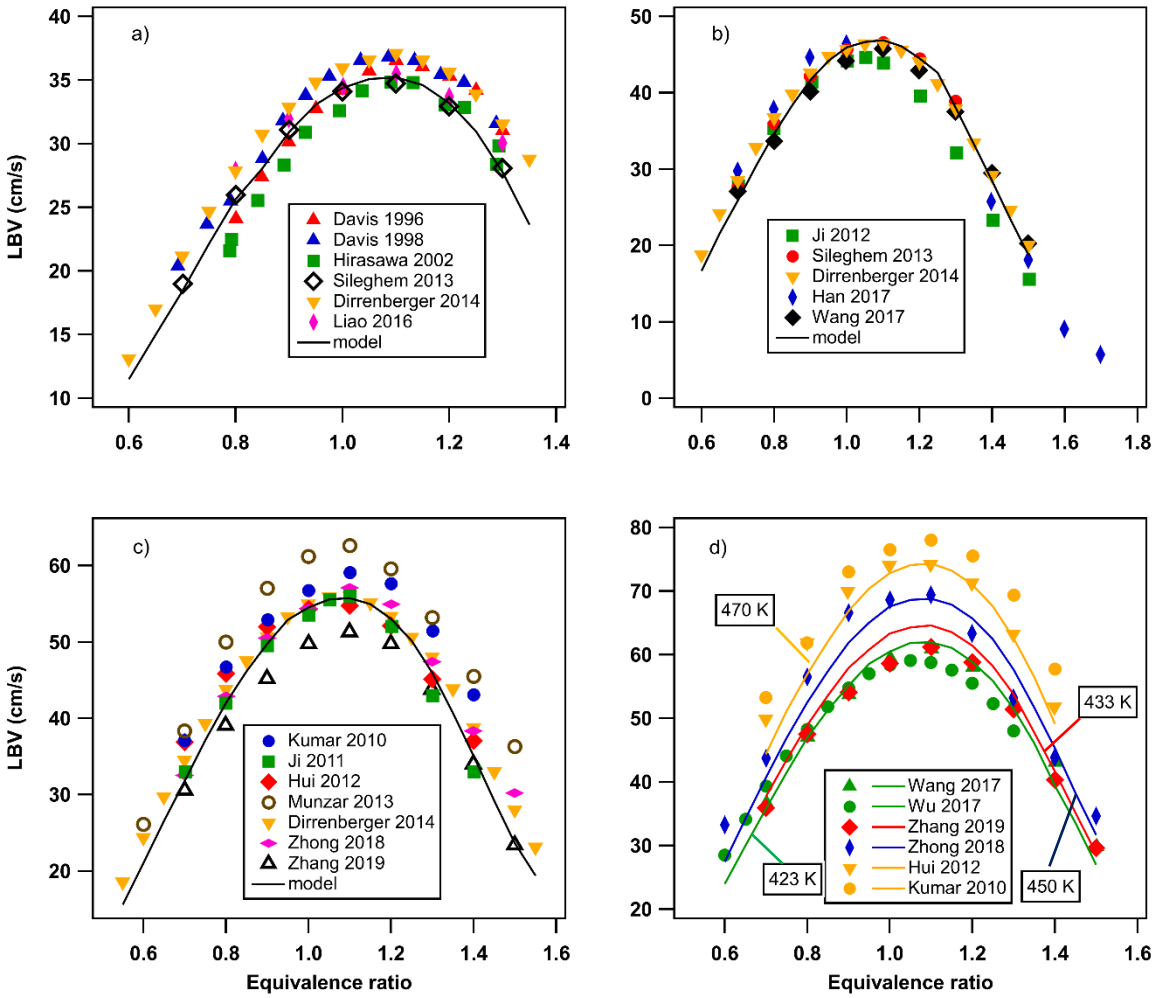

Figure S25: Validation on laminar burning velocities under atmospheric pressure for a fresh gas temperature a) of 298 K [12–17], b) around 358 K [15,16,18–20], c) around 398 K [16,21–26], d) higher than 398 K [20,21,23,25–27].

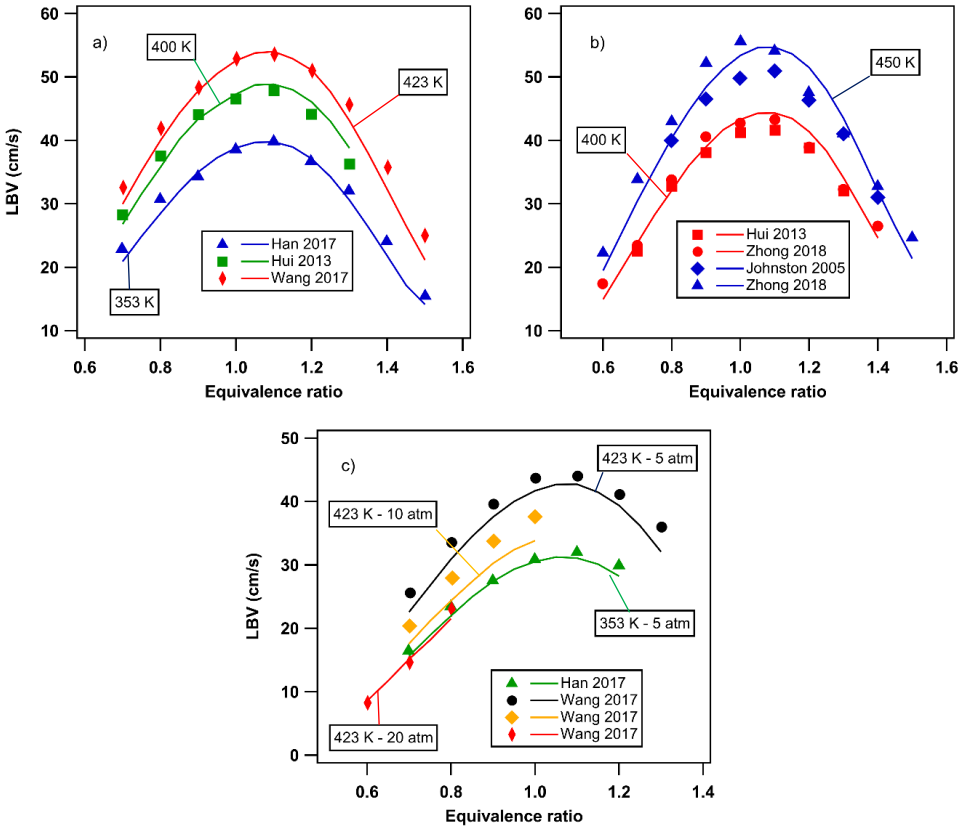

Figure S26: Validation on laminar burning velocities under a) 2 atm [19,20,28], b) 3 atm [25,25,28,29], c) pressure higher than 5 atm [19,20].

3.2/ Validation on existing data of xylene isomers

- **Species profiles in Jet Stirred Reactor**

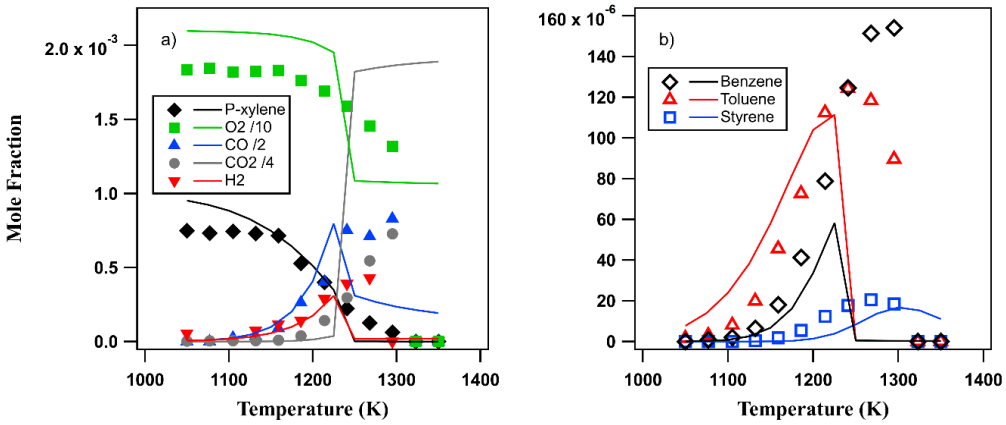

Figure S27: Validation on experimental mole fraction profiles obtained by Gaïl et al. [30] during the oxidation of p-xylene in JSR at Φ=0.5 (τ=0.1 s, P=1 atm). a) fuel and main light species, b) main aromatic compounds.

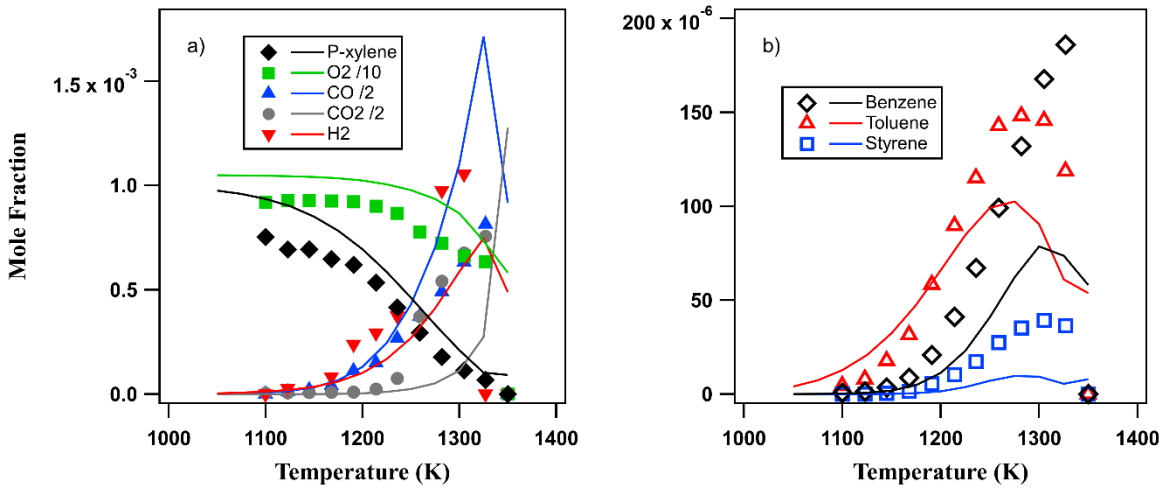

Figure S28: Validation on experimental mole fraction profiles obtained by Gaïl et al. [30] during the oxidation of p-xylene in JSR at Φ=1 (τ=0.1 s, P=1 atm). a) fuel and main light species, b) main aromatic compounds.

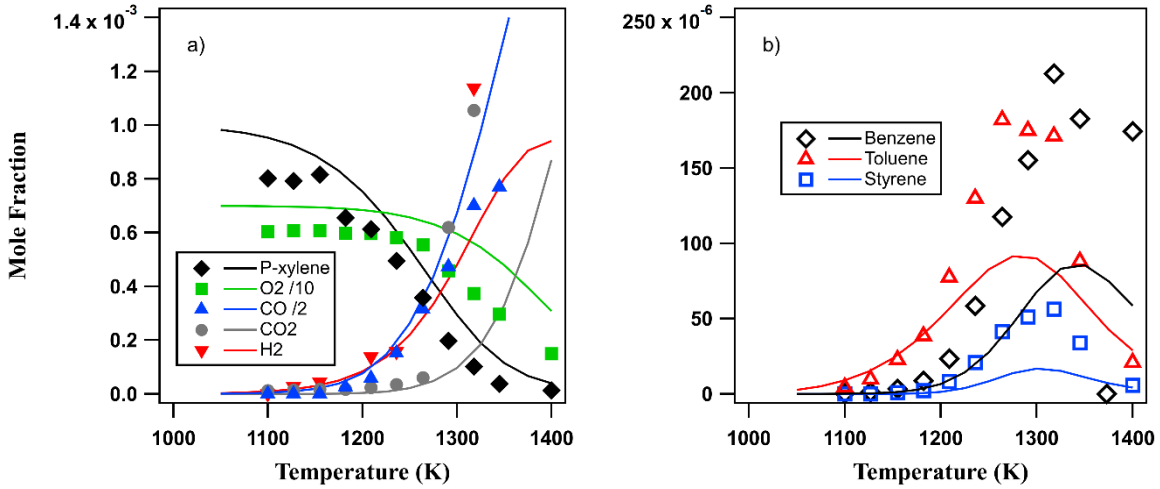

Figure S29: Validation on experimental mole fraction profiles obtained by Gaïl et al. [30] during the oxidation of p-xylene in JSR at Φ=1.5 (τ=0.1s, P=1 atm). a) fuel and main light species, b) main aromatic compounds.

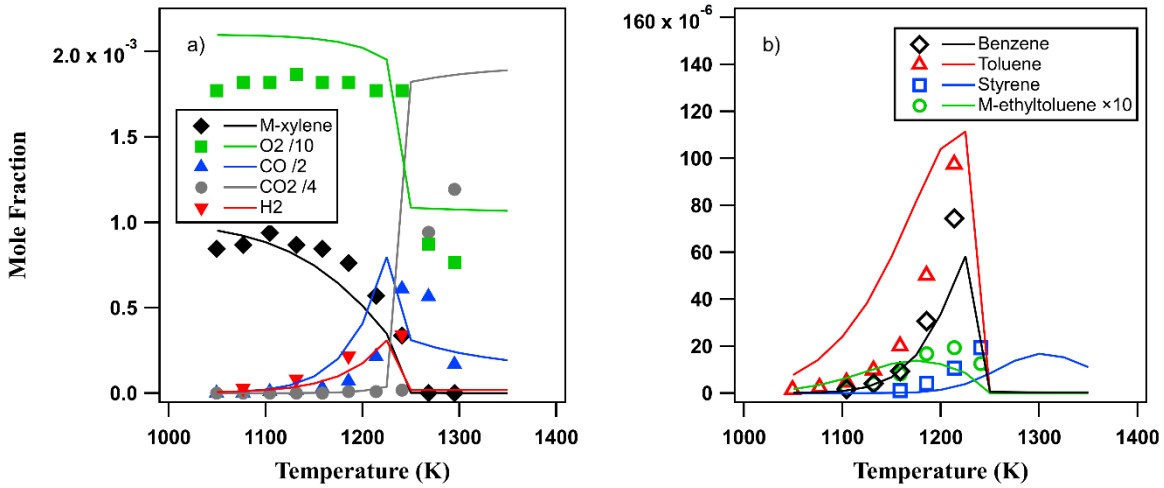

Figure S30: Validation on experimental mole fraction profiles obtained by Gaïl et al. [31] during the oxidation of m-xylene in JSR at Φ=0.5 (τ=0.1 s, P=1 atm). a) fuel and main light species, b) main aromatic compounds.

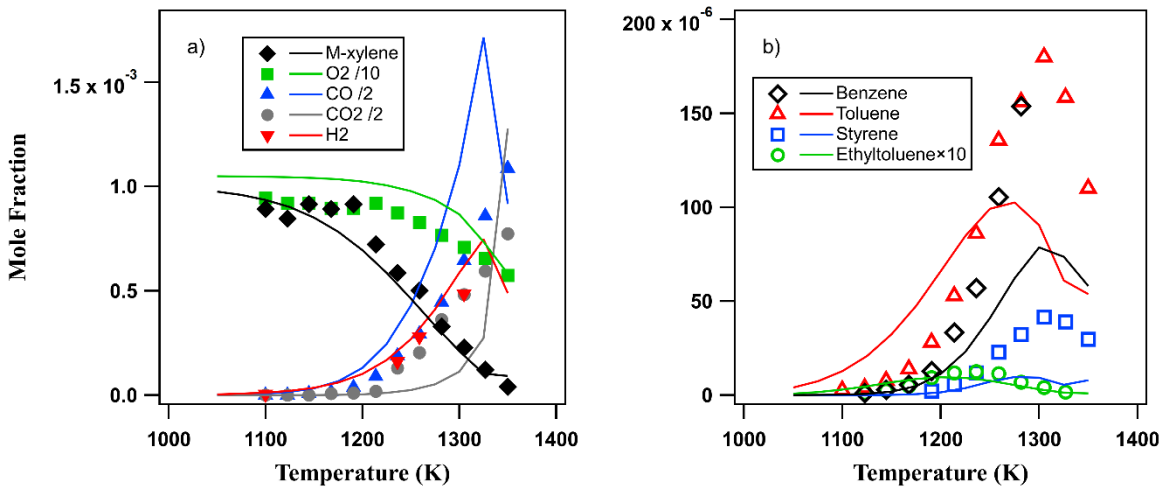

Figure S31: Validation on experimental mole fraction profiles obtained by Gaïl et al. [31] during the oxidation of m-xylene in JSR at Φ=1 (τ=0.1 s, P=1 atm). a) fuel and main light species, b) main aromatic compounds.

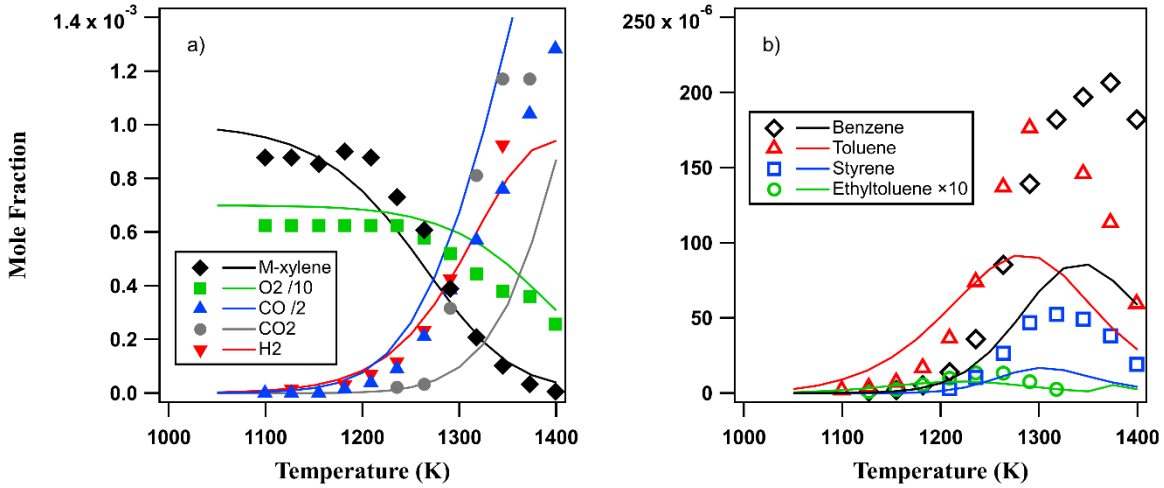

Figure S32: Validation on experimental mole fraction profiles obtained by Gaïl et al. [31] during the oxidation of m-xylene in JSR at Φ=1.5 (τ=0.1 s, P=1 atm). a) fuel and main light species, b) main aromatic compounds.

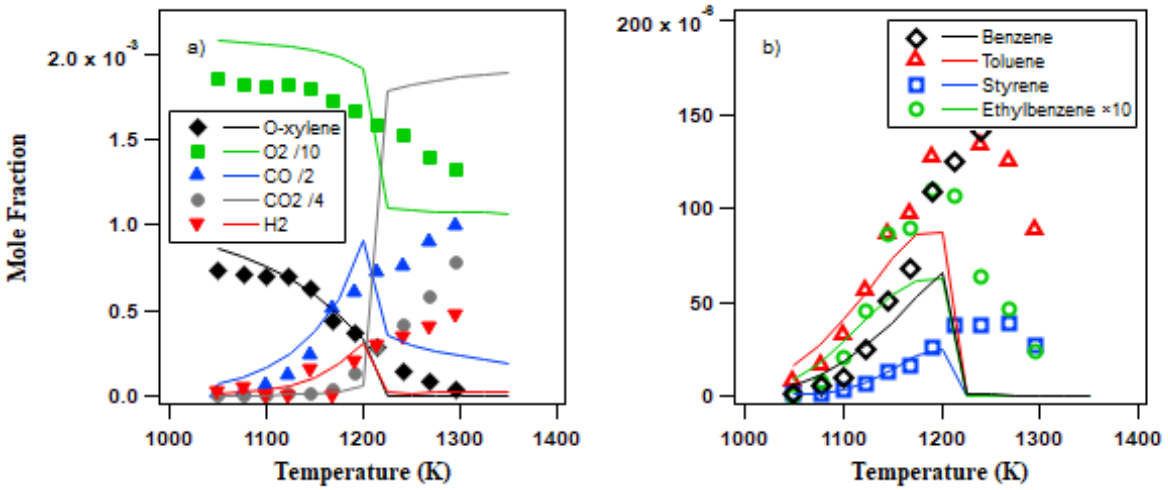

Figure S33: Validation on experimental mole fraction profiles obtained by Gaïl et al. [32] during the oxidation of o-xylene in JSR at Φ=0.5 (τ=0.1 s, P=1 atm). a) fuel and main light species, b) main aromatic compounds.

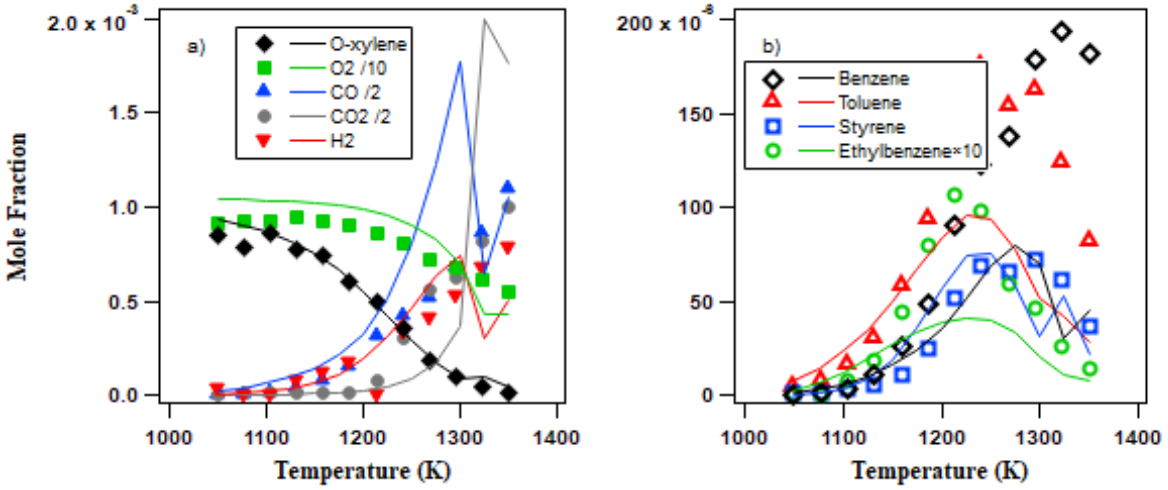

Figure S34: Validation on experimental mole fraction profiles obtained by Gaïl et al. [32] during the oxidation of o-xylene in JSR at Φ=1 (τ=0.1 s, P=1 atm). a) fuel and main light species, b) main aromatic compounds.

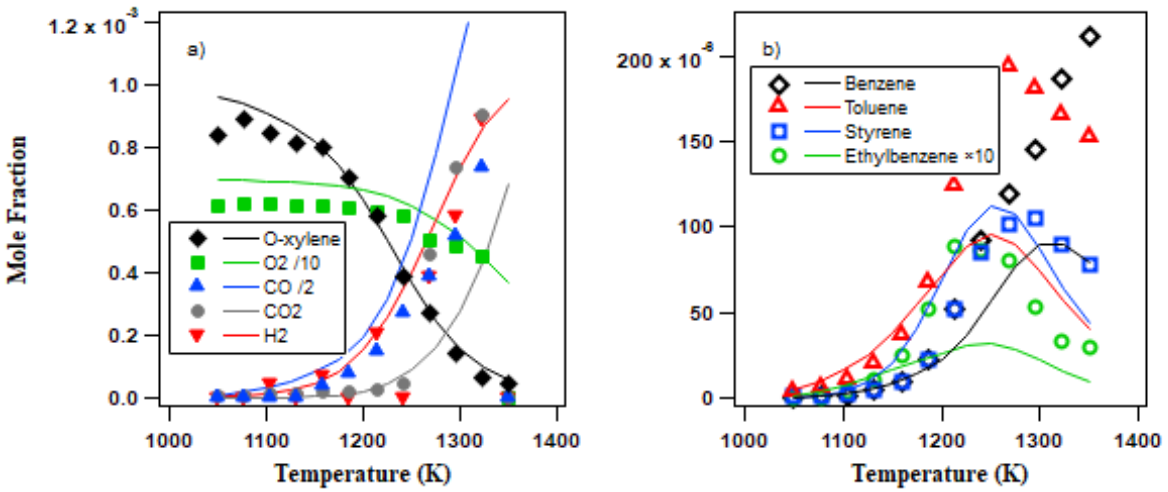

Figure S35: Validation on experimental mole fraction profiles obtained by Gaïl et al. [32] during the oxidation of o-xylene in JSR at Φ=1.5 (τ=0.1 s, P=1 atm). a) fuel and main light species, b) main aromatic compounds.

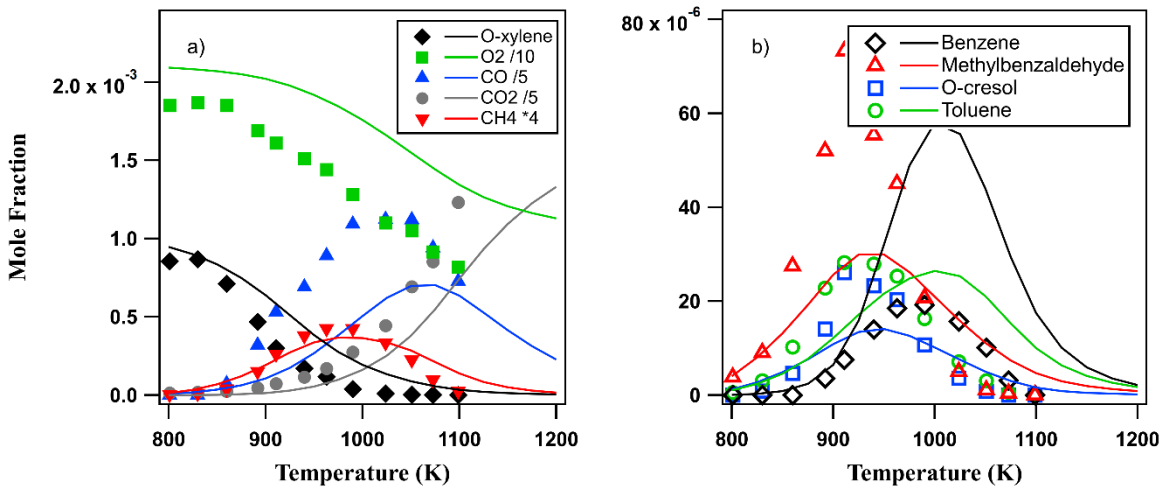

Figure S36: Validation on experimental mole fraction profiles obtained by Yuan et al. [33] during the oxidation of o-xylene in JSR at Φ=0.5 (τ=0.5 s, P=10 atm). a) fuel and main light species, b) main aromatic compounds.

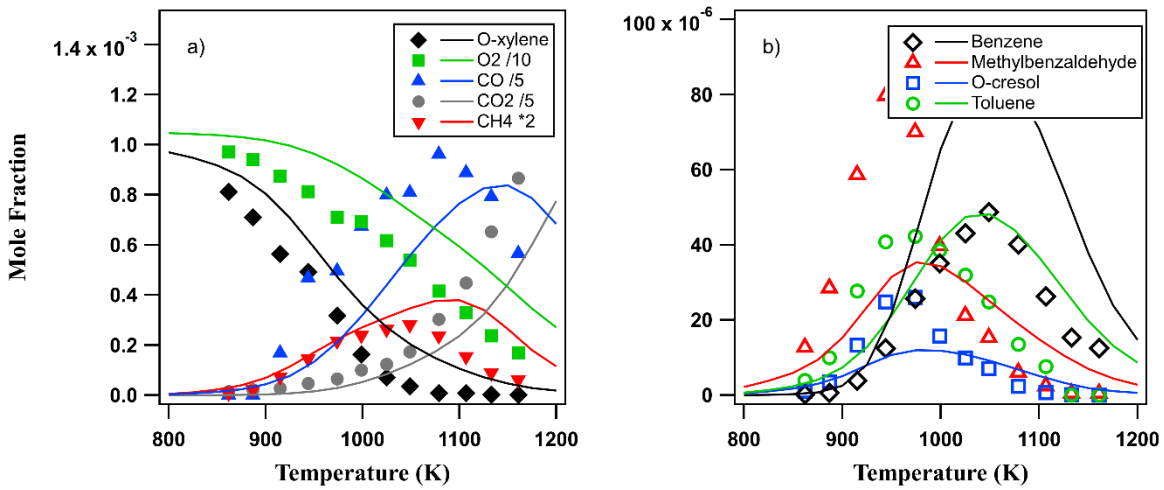

Figure S37: Validation on experimental mole fraction profiles obtained by Yuan et al. [33] during the oxidation of o-xylene in JSR at Φ=1 (τ=0.5 s, P=10 atm). a) fuel and main light species, b) main aromatic compounds.

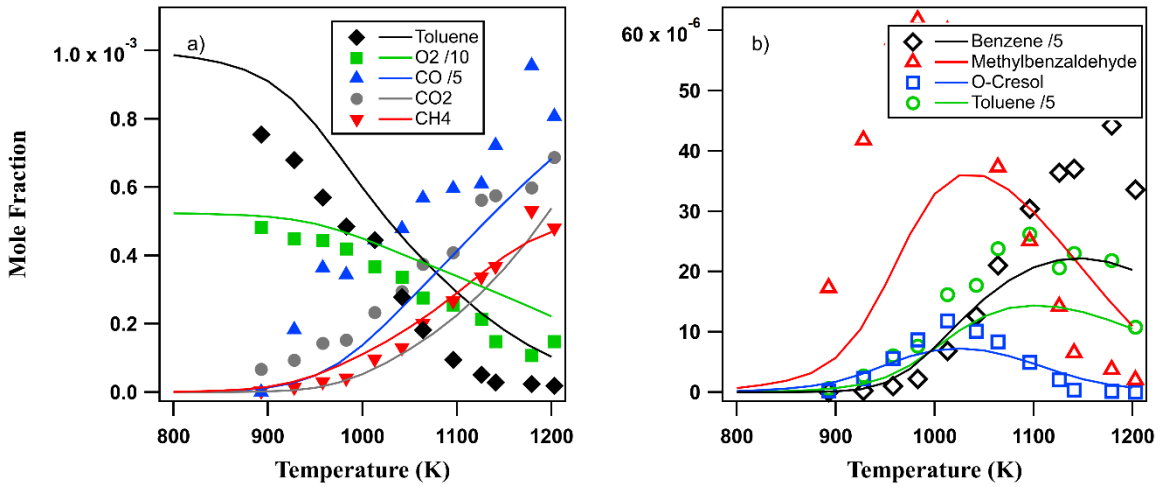

Figure S38: Validation on experimental mole fraction profiles obtained by Yuan et al. [33] during the oxidation of o-xylene in JSR at Φ=2 (τ=0.5 s, P=10 atm). a) fuel and main light species, b) main aromatic compounds.

- **Ignition delay times**

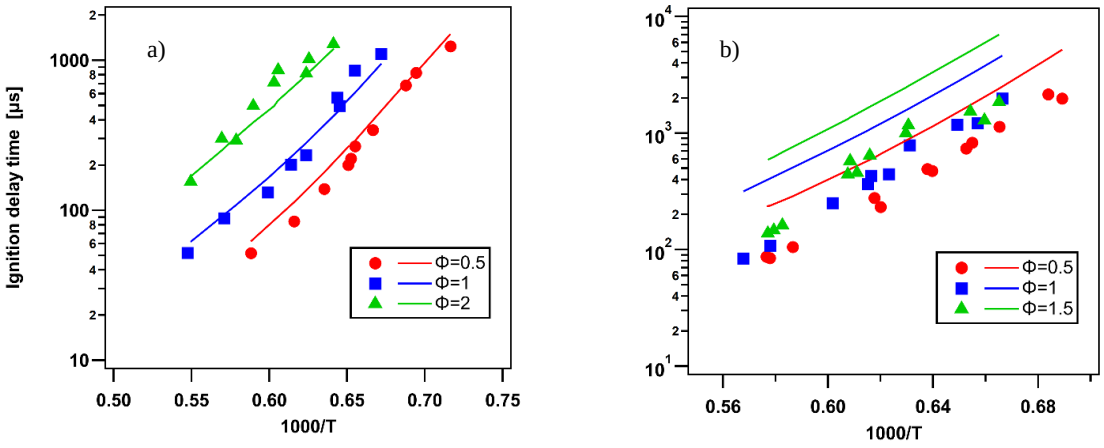

Figure S39: Validation on experimental ignition delay times obtained in shock tube by Gaïl et al. [30,32] around atmospheric pressure for a) o-xylene and b) p-xylene as fuels.

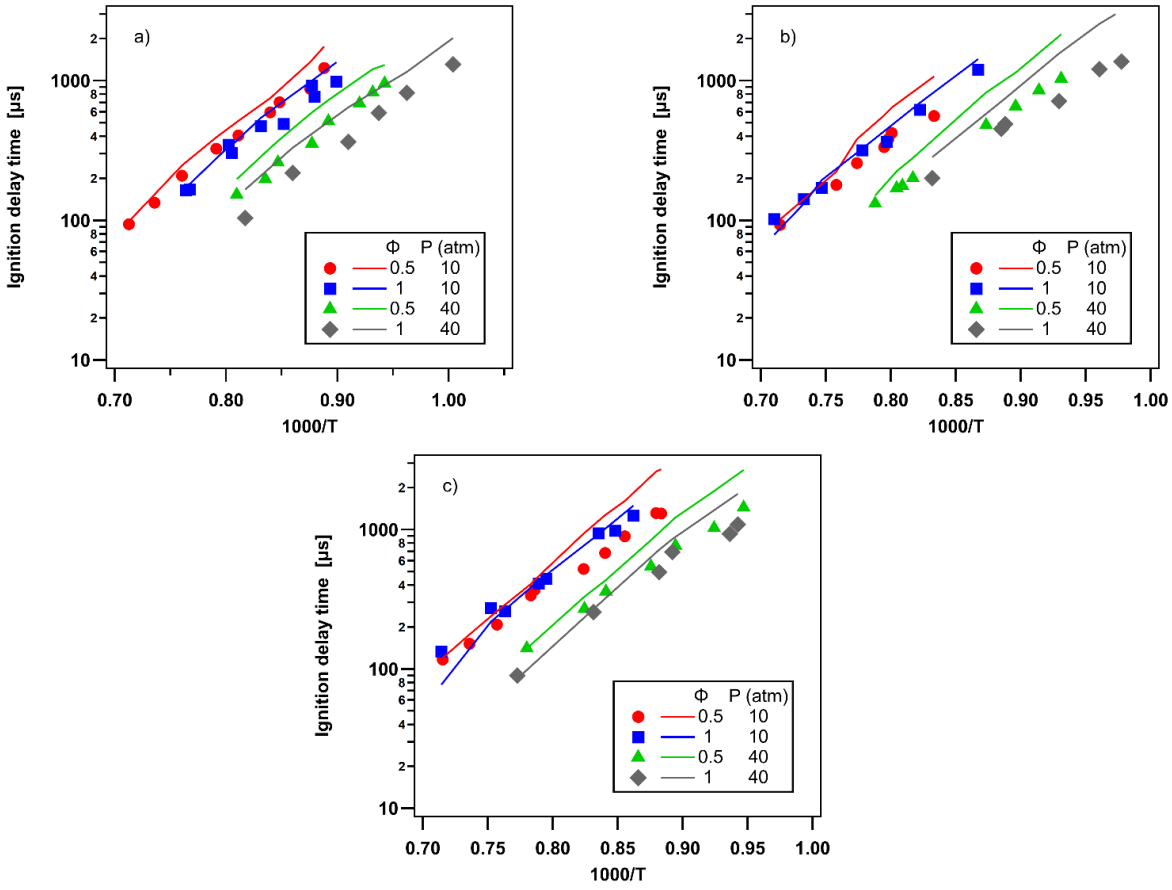

Figure S40: Validation on ignition delay time measurements obtained by Shen et al. [34] in shock tube for a) o-xylene, b) m-xylene, c) p-xylene as fuels.

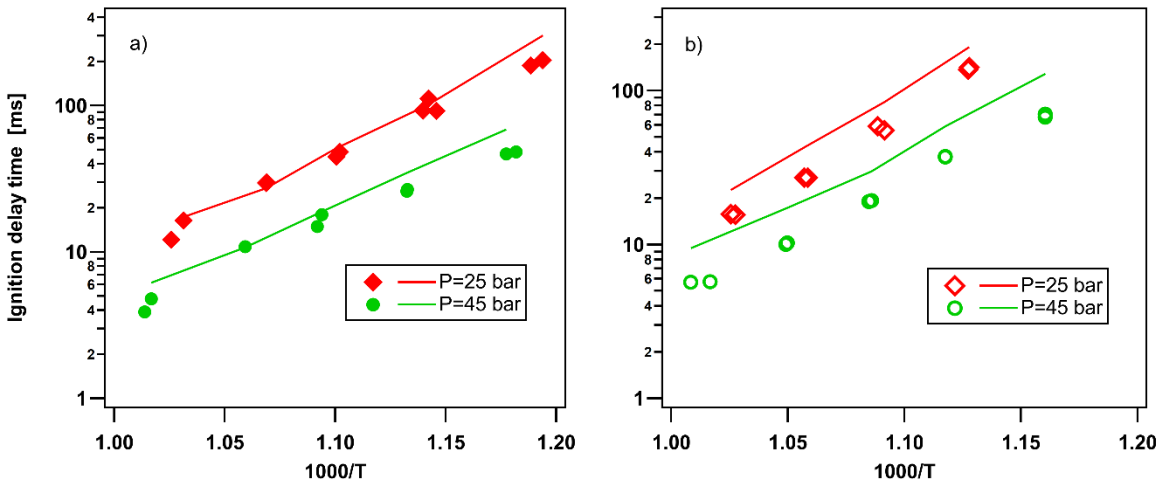

Figure S41: Validation on ignition delay time measurements obtained by Kukkadapu et al. [7] in a rapid compression machine with o-xylene as a fuel for a) Φ=1, b) Φ=0.5.

- **Mole fraction profiles in shock tube**

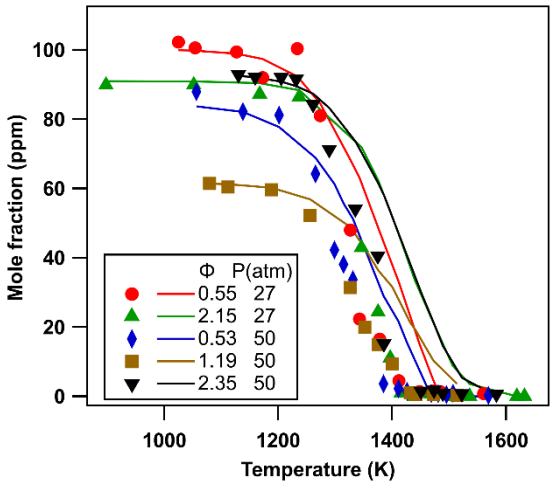

Figure S42: Validation on the fuel consumption mole profiles obtained by Gudiyella et al. [35] in shock tube during the oxidation of m-xylene.

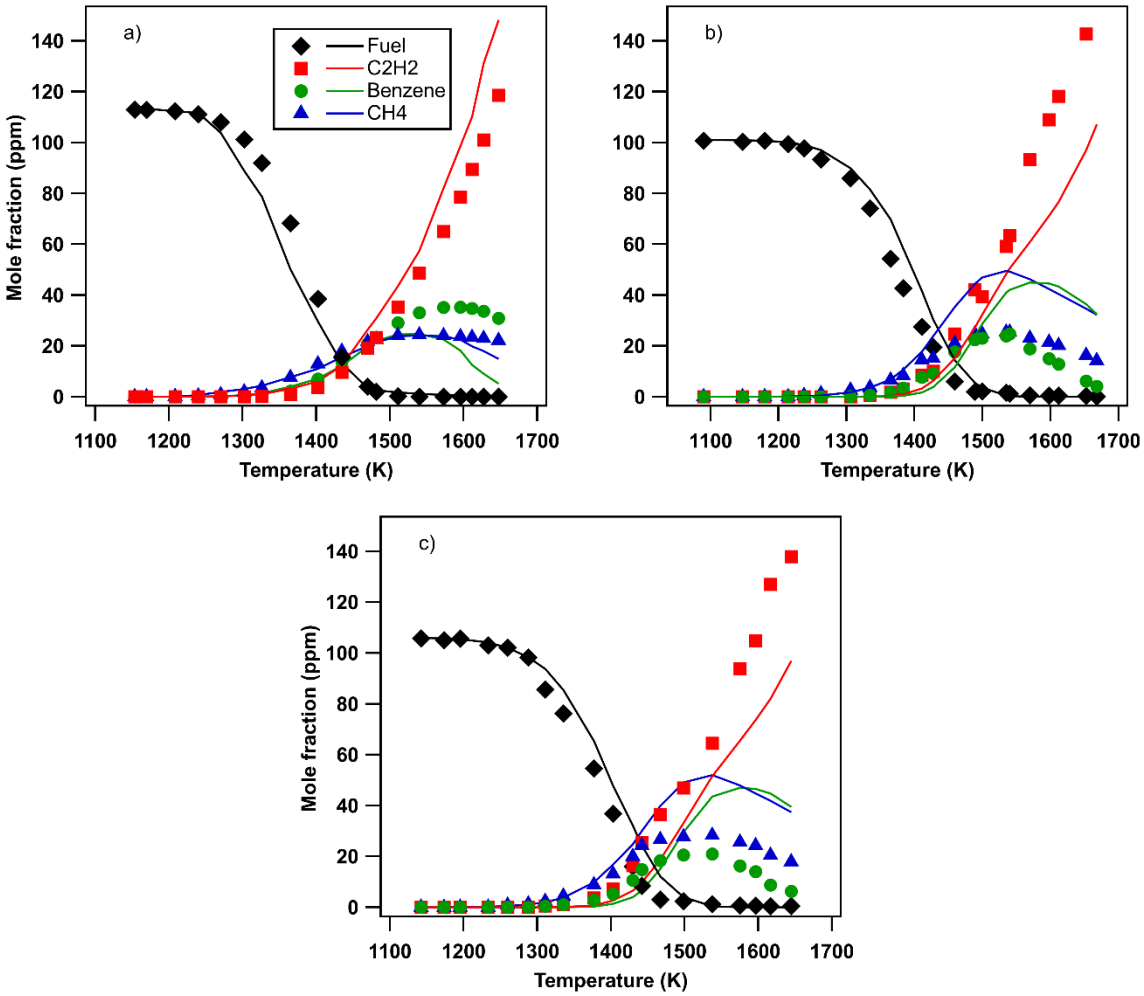

Figure S43: Validation on main experimental mole fraction profiles obtained by Sun et al. [36] in shock tube during the pyrolysis of a) o-xylene, b) m-xylene, c) p-xylene.

- **Plug Flow Reactor**

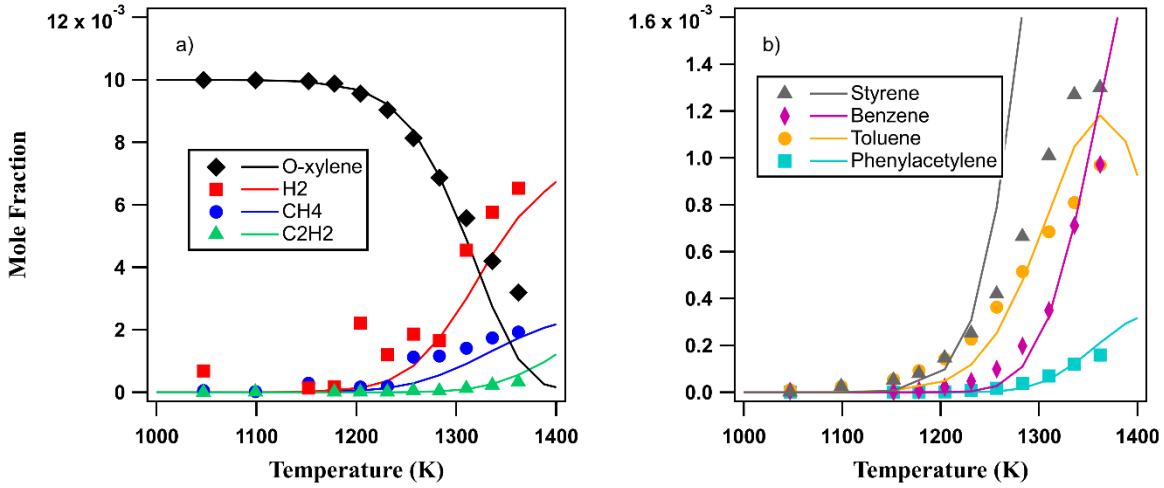

Figure S44: Validation on experimental mole fraction profiles obtained by Yuan et al. [33] during the pyrolysis of o-xylene in a plug flow reactor under 1 atm, a) fuel and main light species, b) main aromatic compounds.

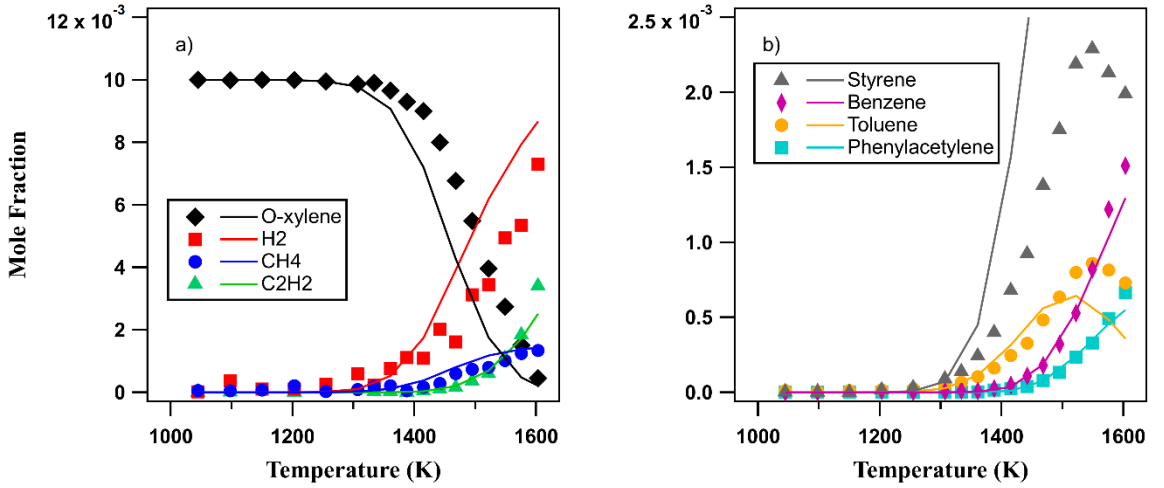

Figure S45: Validation on experimental mole fraction profiles obtained by Yuan et al. [33] during the pyrolysis of o-xylene in a plug flow reactor under 4.10^{-2} atm, a) fuel and main light species, b) main aromatic compounds.

- **Flame structure**

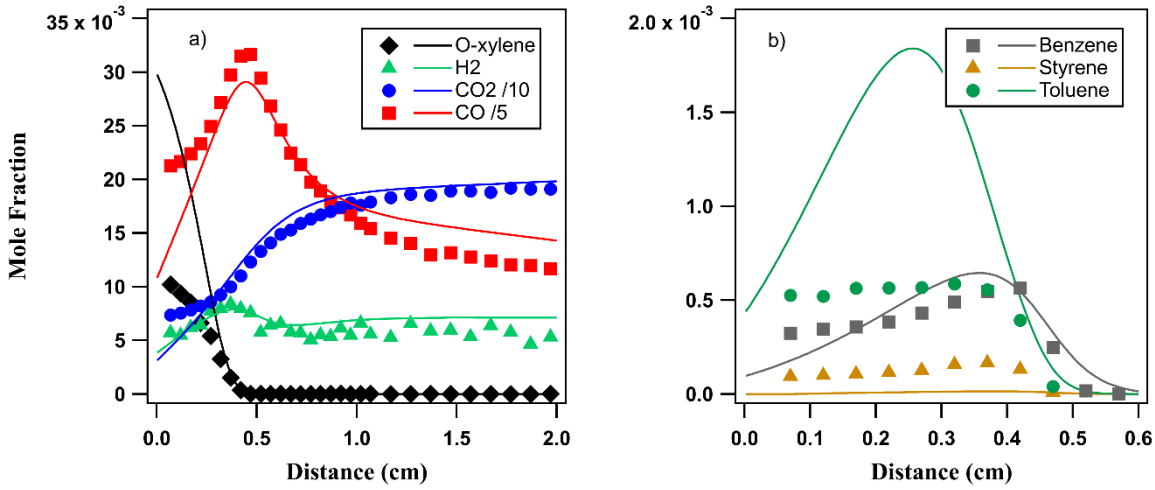

Figure S46: Validation on mole fraction profiles obtained by Zhao et al. [37] in a o-xylene - O_2 - Ar flame at Φ=0.75 under 4.10^{-2} bar, a) fuel and main light species, b) main aromatic compounds.

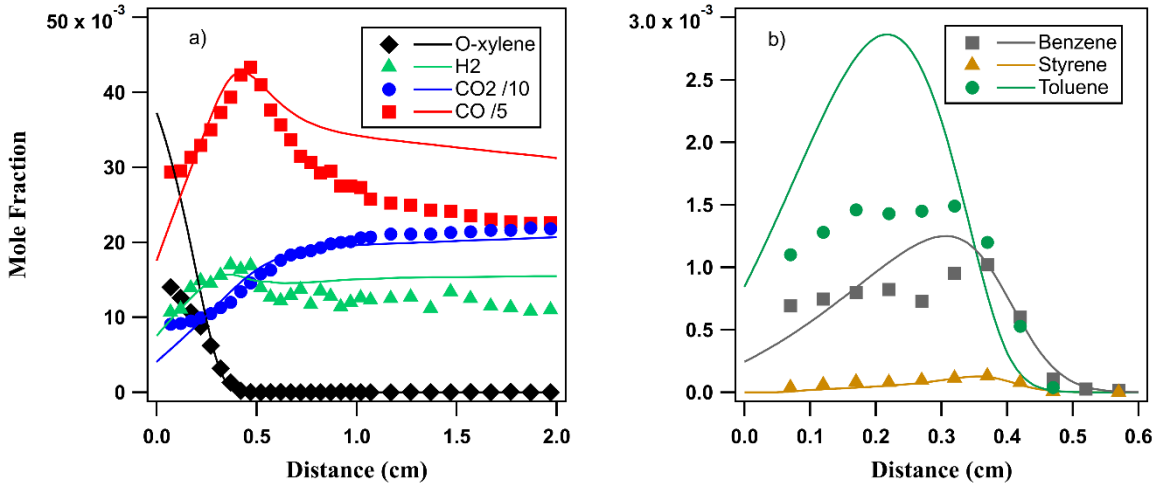

Figure S47: Validation on mole fraction profiles obtained by Zhao et al. [37] in a O-xylene - O_2 - Ar flame at Φ=1 under 4.10^{-2} bar, a) fuel and main light species, b) main aromatic compounds.

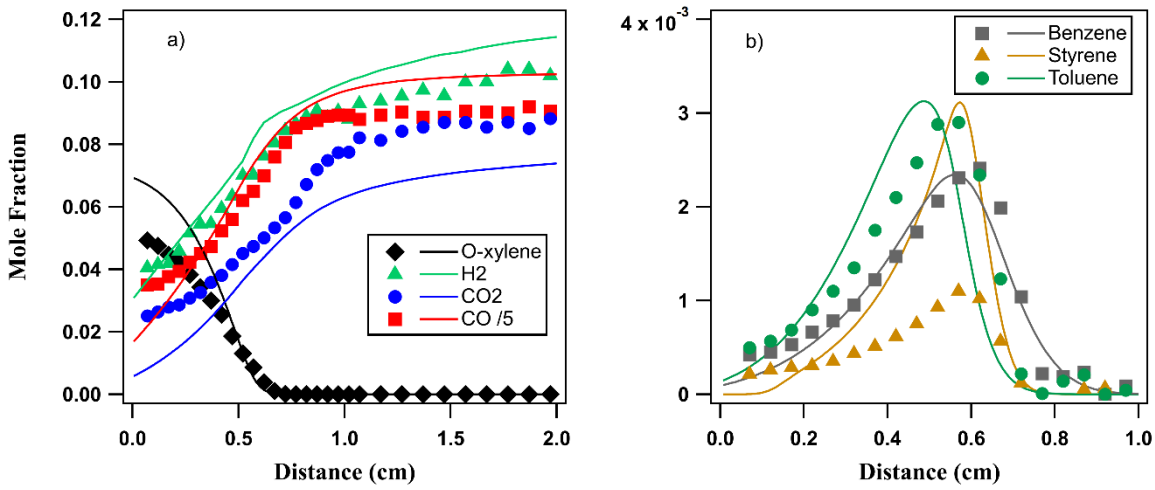

Figure S48: Validation on mole fraction profiles obtained by Zhao et al. [37] in a O-xylene - O_2 - Ar flame at Φ=1.79 under 4.10^{-2} bar, a) fuel and main light species, b) main aromatic compounds.

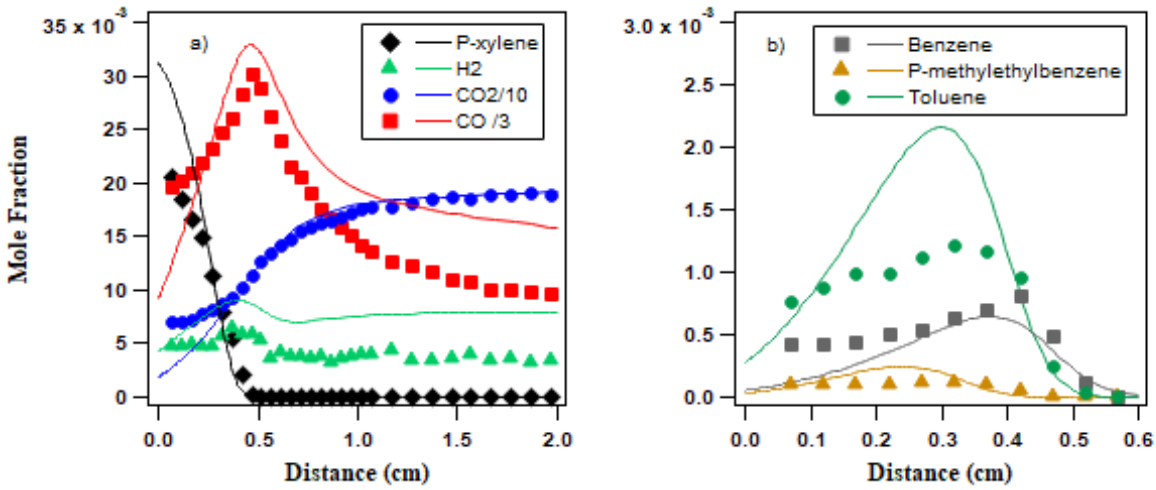

Figure S49: Validation on mole fraction profiles obtained by Yuan et al. [38] in a P-xylene - O_2 - Ar flame at Φ=0.75 under 4.10^{-2} atm, a) fuel and main light species, b) main aromatic compounds.

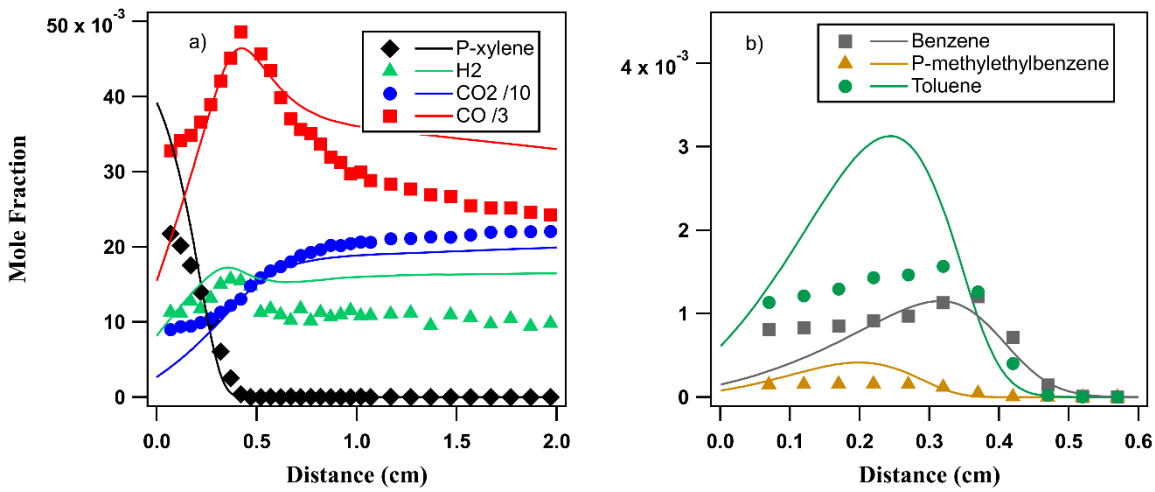

Figure S50: Validation on mole fraction profiles obtained by Yuan et al. [38] in a P-xylene - O_2 - Ar flame at Φ=1 under 4.10^{-2} atm, a) fuel and main light species, b) main aromatic compounds.

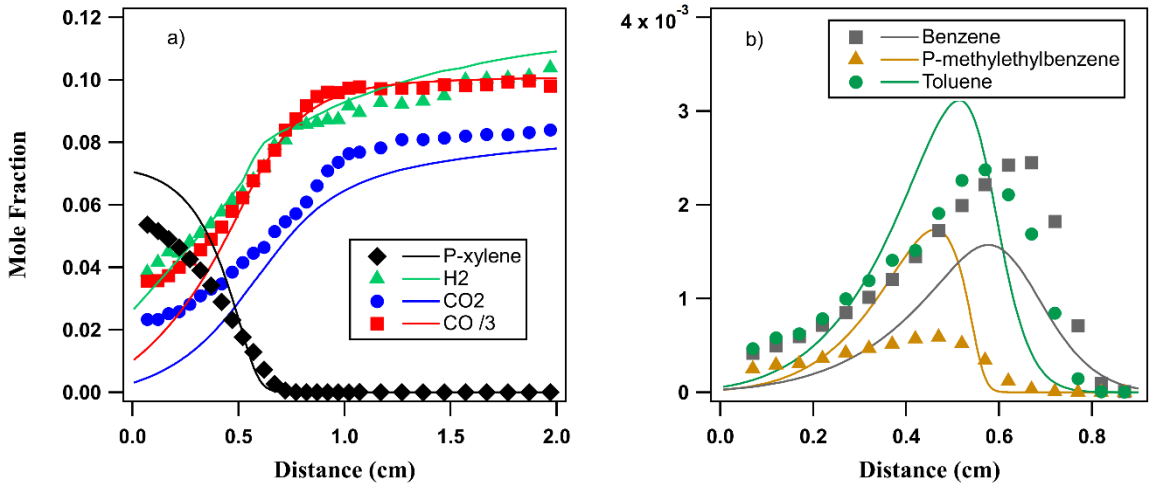

Figure S51: Validation on mole fraction profiles obtained by Yuan et al. [38] in a P-xylene - O_2 - Ar flame at Φ=1.79 under 4.10^{-2} atm, a) fuel and main light species, b) main aromatic compounds.

- **Laminar Burning Velocities**

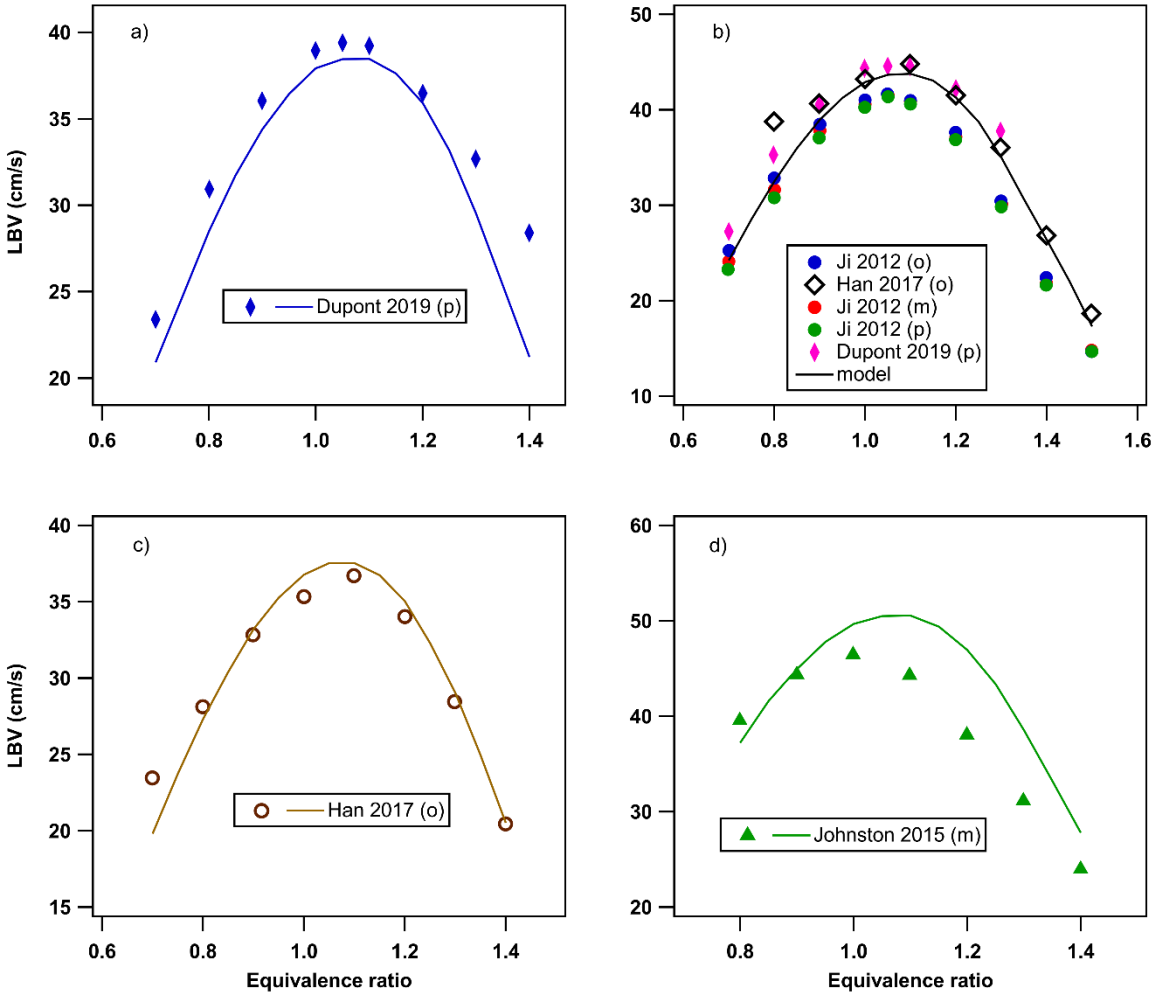

Figure S52: Validation on laminar burning velocities a) under atmospheric pressure and for fresh gas temperature of 328 K [39], b) under atmospheric pressure and for fresh gas temperature of 353 K [18,19,39], c) under 2 atm and for fresh gas temperature of 353 K [19], d) under 3 atm and for fresh gas temperature of 450 K [29]. The considered isomers (o, m or p) are indicated in legends.

3.3/ Comments on the validations of the COLIBRI model on literature data

An overall good agreement is observed on a large set of experimental data with simulations made using the COLIBRI model. The used experimental results are species profiles in JSR, tubular reactors, shock tubes and flames, as well as ignition delay times and laminar burning velocities measured with different kinds of facility.

Concerning the comparisons with JSR experiments performed at Orléans under atmospheric pressure (Figures S2-4, S27-35), the agreement is generally acceptable (similar temperature evolution and predicted and simulated maximum mole fractions within a factor 1.5); however, benzene mole fraction is underestimated by a factor of 2 whatever the equivalence ratio during the oxidation of toluene and it is also the case for all main arenes (toluene, benzene, styrene) during the oxidation of xylenes. Finally, during the oxidation of xylenes, CO_2 starts to be formed at the same temperature as for experiments but is not formed fast enough. At higher pressure and under lean condition (Figure S5, S36), O_2 is slightly overestimated.

Concerning comparisons against tubular reactor data (Figures S16-19, S44-45), a good agreement is found against literature data; however, a 50 K-shift of temperature is observed during the pyrolysis of o-xylene under low pressure (Figure S45).

In flame, whatever the condition, deviations can be observed concerning the fuel consumption and main products formation close to the burner (Figures S20-24, S46-51). However, species predictions are dependent on the given temperature profile in the flame on which there is a significant uncertainty (e.g.: 100K in Li et al. [11,40] studies) what has a strong impact on the start of reactivity. So, it is difficult to attribute the deviations either to the detailed kinetic model or to the temperature measurements.

During the validation against species profiles measured in shock tube (Figures S13-15, S42-43), there is generally a delay on the start of fuel consumption compared to experiments,

between 50 and 100 K (Figures S13-15, S42). Only validation against Sun et al. [36] results (see Figure S42) shows a good agreement concerning the fuel consumption.

The agreement for ignition delay times is also reasonable (Figures S8-12, S39-41); however, a few of them are a little bit overestimated, most of them under lean condition, but no clear tendency is observed on the whole set of data, numerical and experimental results are close in all other cases whatever the pressure, the temperature and the chemical composition.

Concerning literature data for laminar burning velocities (Figures S25-26, S52), some of them obtained under the same conditions are sometimes scattered: deviations higher than 10 cm/s are observed in some conditions (e.g. toluene flame with fresh gas at 398K under atmospheric pressure on Figure 24 c) despite the given uncertainties are always lower than 2 cm/s. Considering laminar burning velocities of toluene, xylenes and other arenes in literature, it appears that measurements performed with a flat flame burner coupled with the heat flux method are the most accurate as the repeatability is excellent and the measured values are between the set of data existing under the same conditions. Globally, the COLIBRI model predicts reasonably the laminar burning velocities of toluene and xylenes. The most significant deviation is seen against the results of Johnston et al. [29] with m-xylene (Figure 51 d) where, contrary to all other conditions, the top value is experimentally reached for Φ=1 rather than Φ=1.1.

4/ Experimental and simulated temperature evolution at the three equivalence ratios of the mole fraction of the fuel and all the products, which were quantified above 10 ppm during the JSR oxidation of the four investigated methylated benzenes

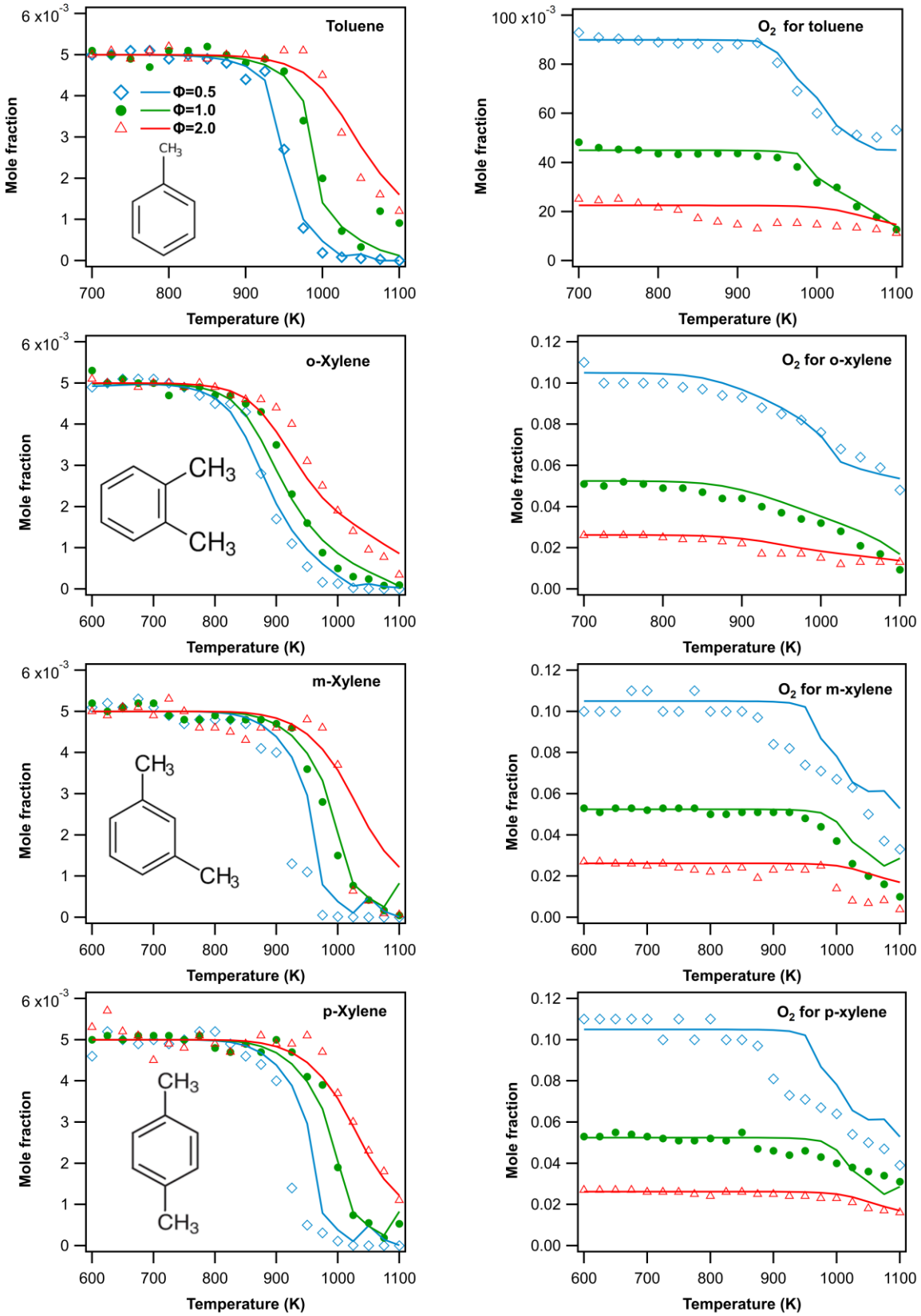

Figure S53: Experimental and simulated temperature evolution at the three equivalence ratios of the mole fraction of the fuel and O_2 for the four reactants.

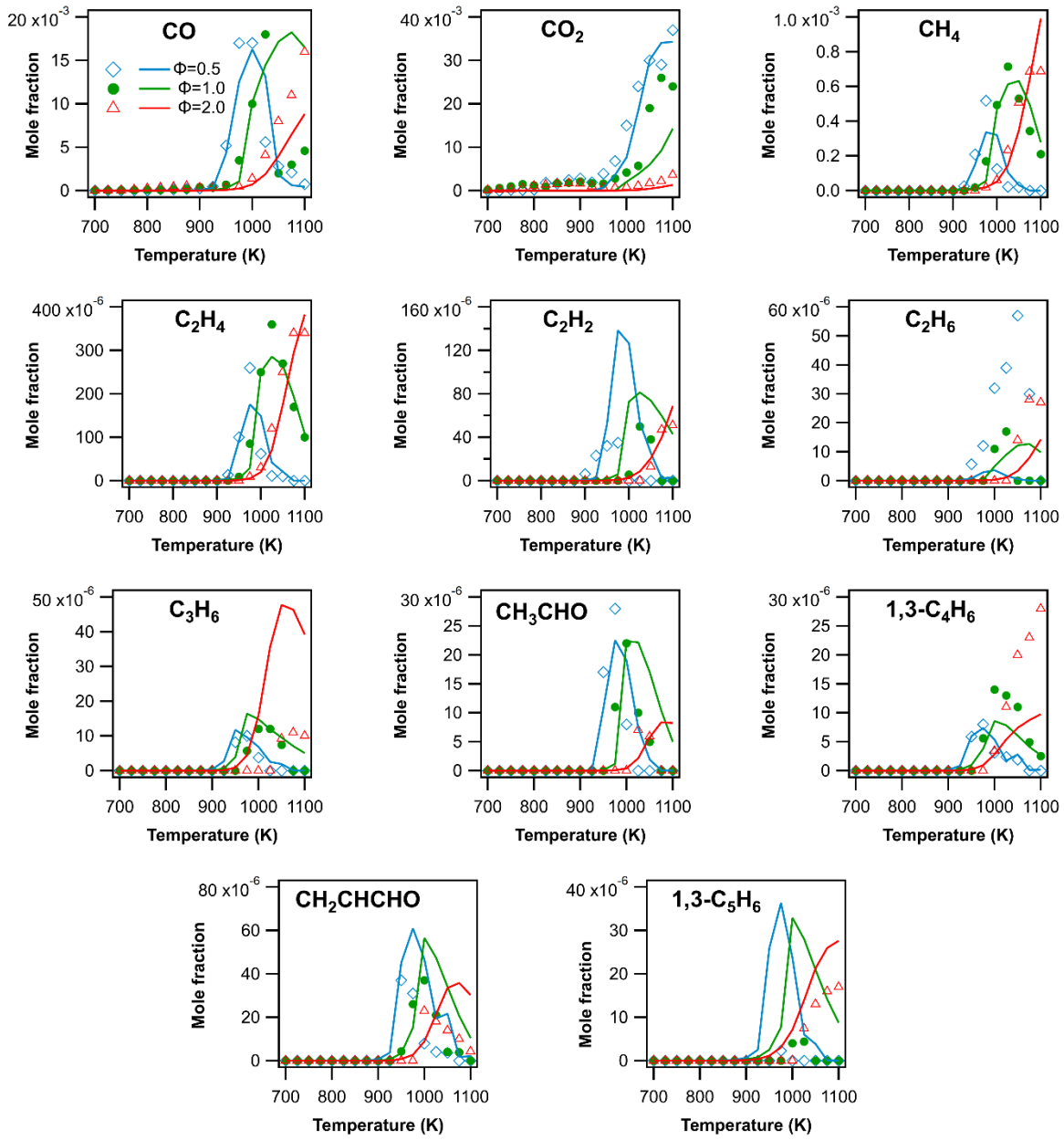

Figure S54: Experimental and simulated temperature evolution at the three equivalence ratios of non-aromatic products during toluene oxidation.

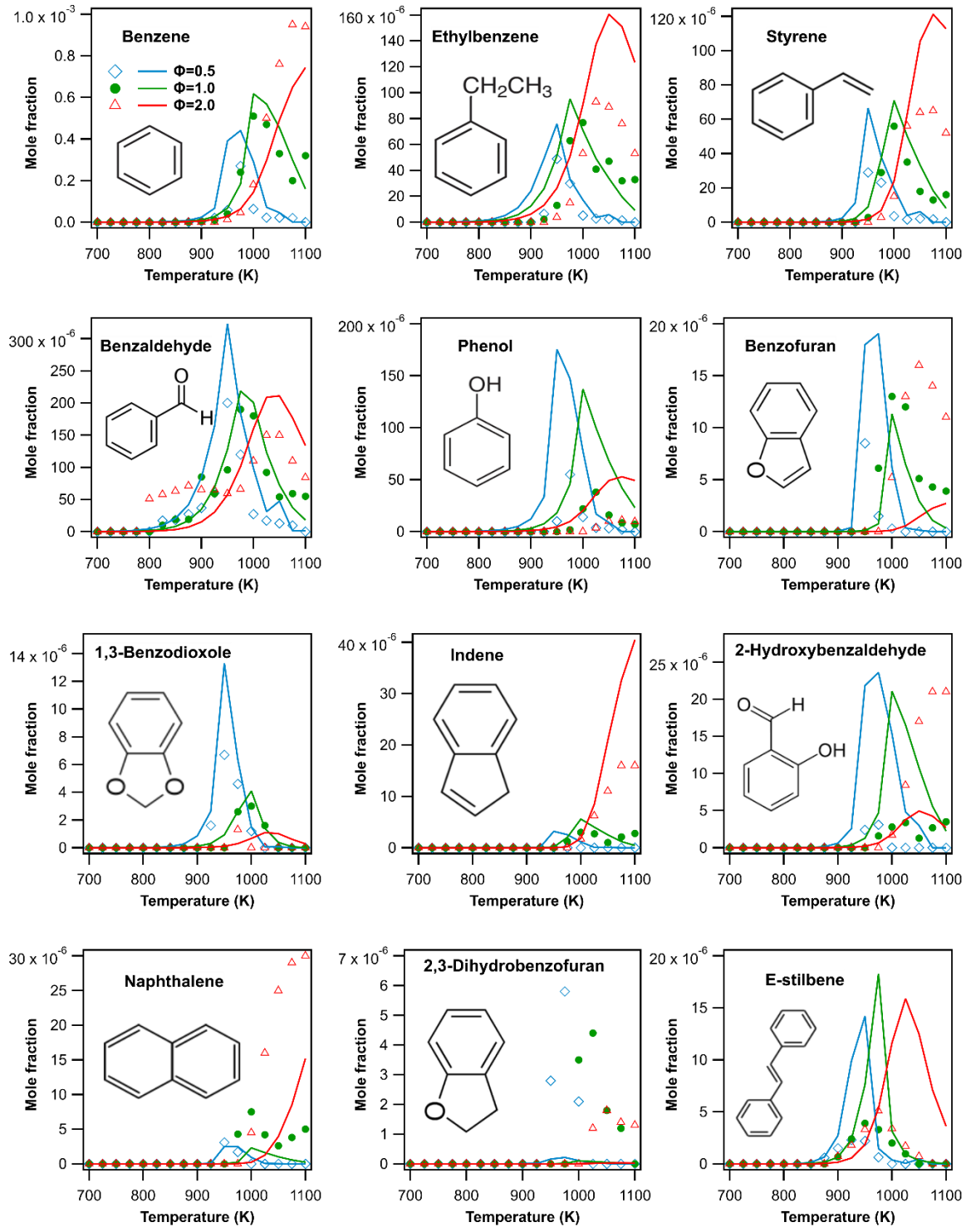

Figure S55: Experimental and simulated temperature evolution at the three equivalence ratios of aromatic products during toluene oxidation.

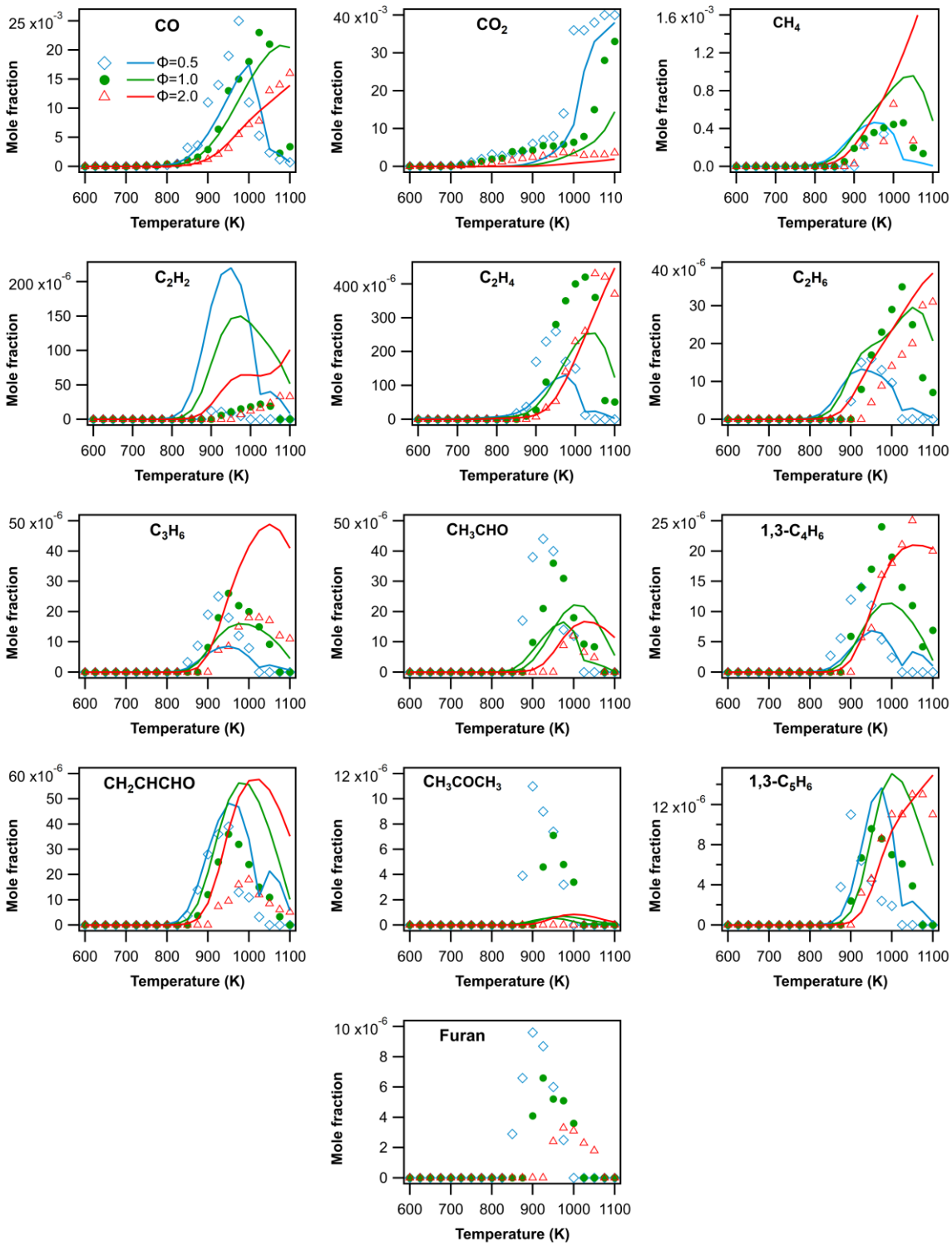

Figure S56: Experimental and simulated temperature evolution at the three equivalence ratios of non-aromatic products during o-xylene oxidation.

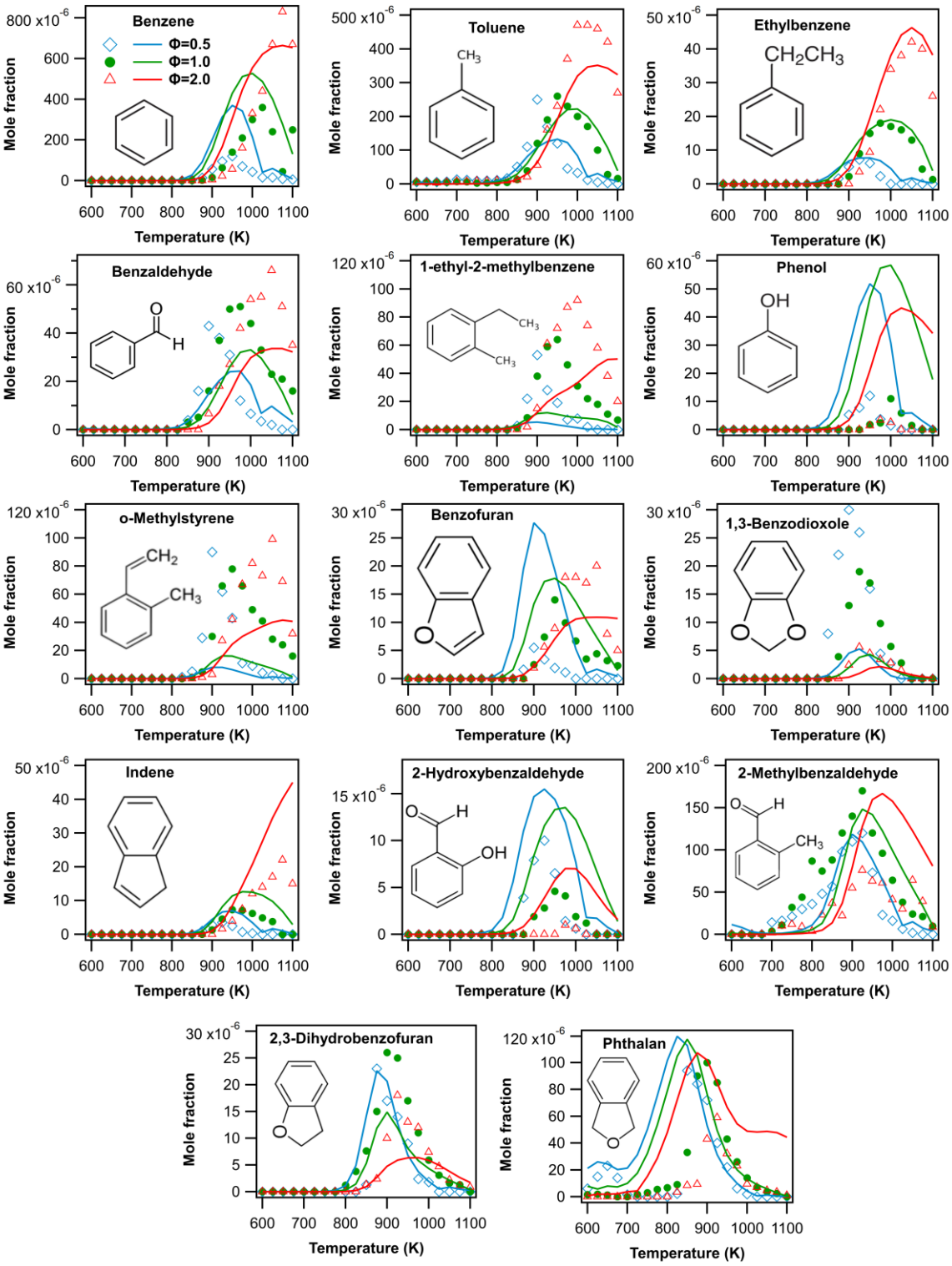

Figure S57: Experimental and simulated temperature evolution at the three equivalence ratios of aromatic products during o-xylene oxidation.

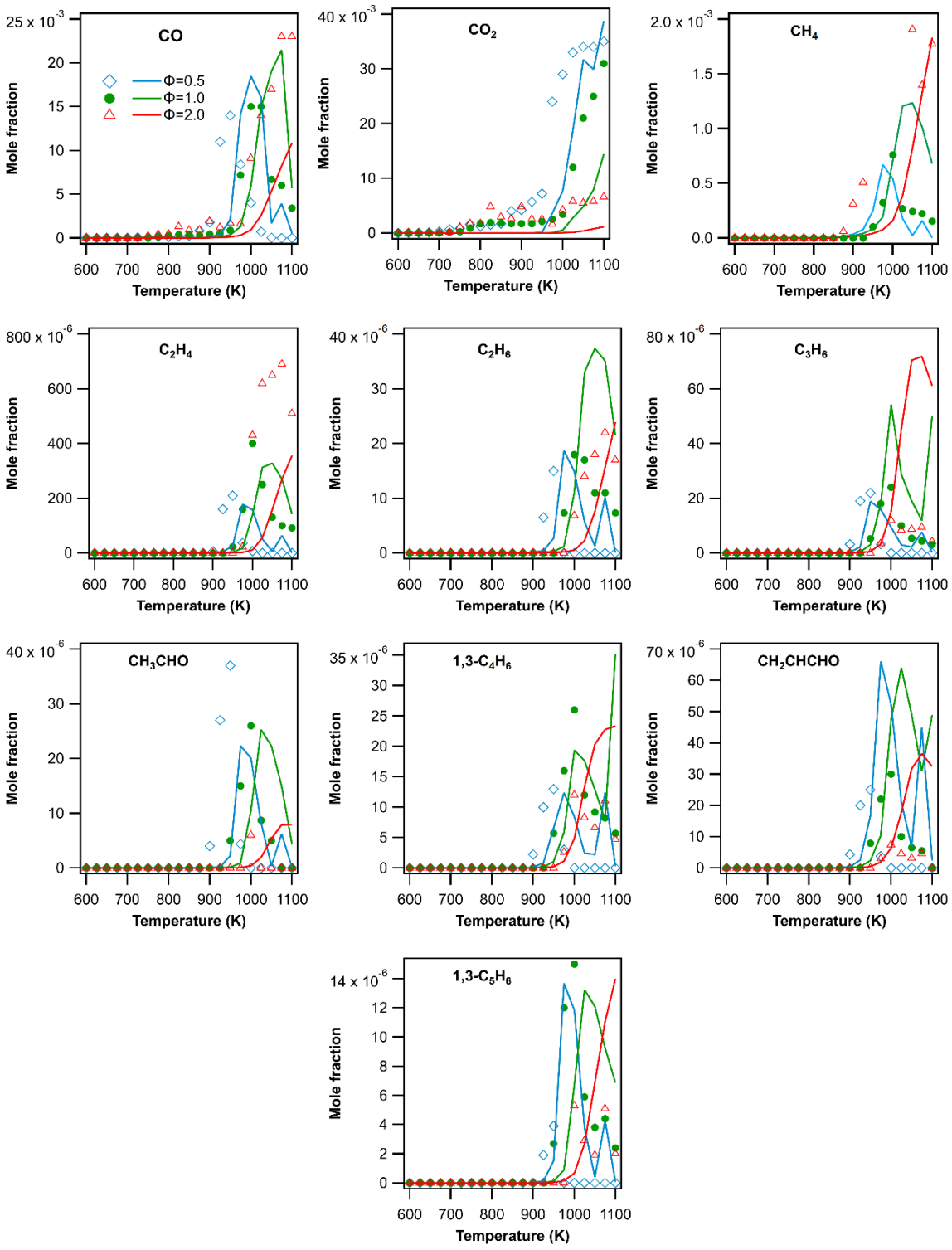

Figure S58: Experimental and simulated temperature evolution at the three equivalence ratios of non-aromatic products during m-xylene oxidation.

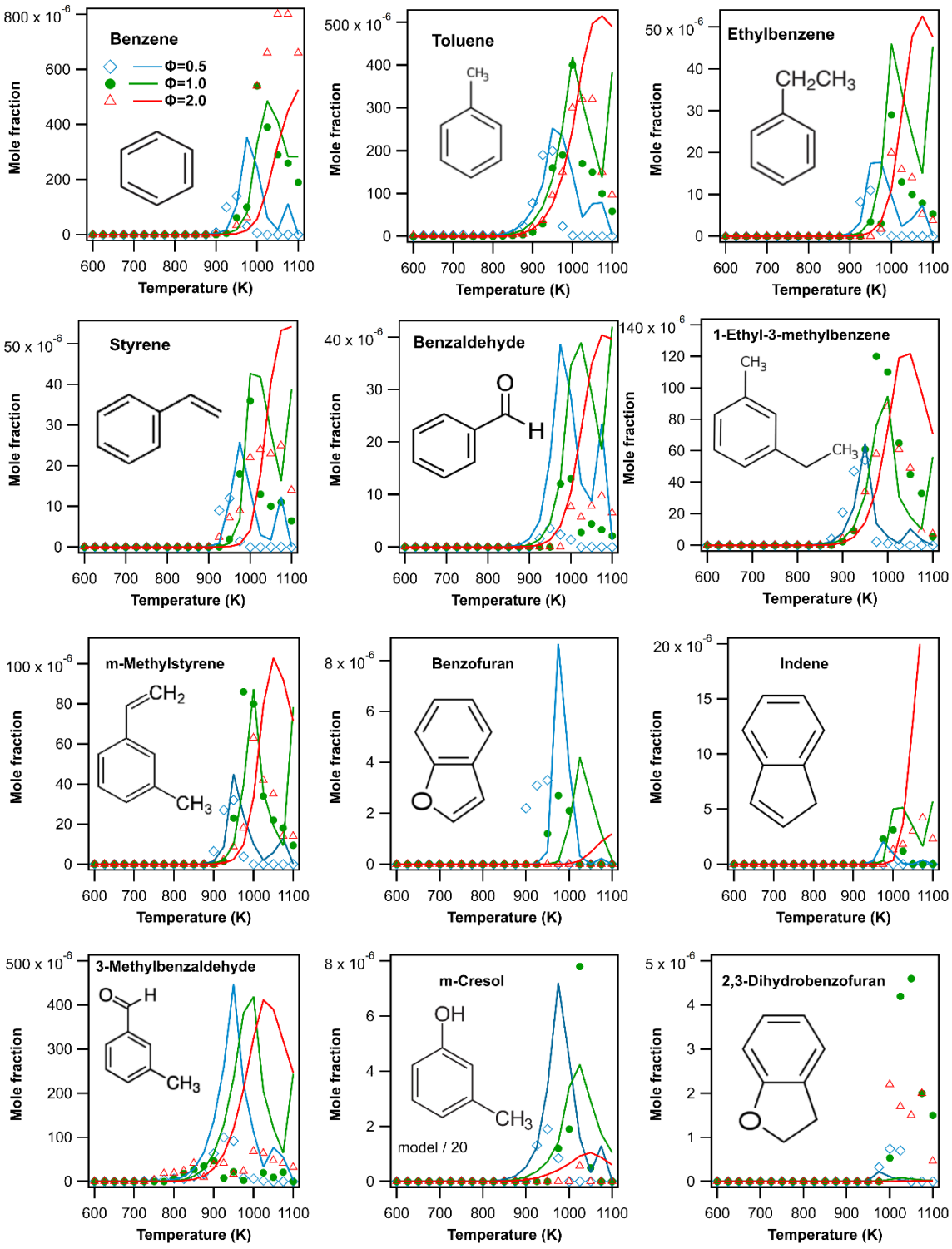

Figure S59: Experimental and simulated temperature evolution at the three equivalence ratios of aromatic products during m-xylene oxidation.

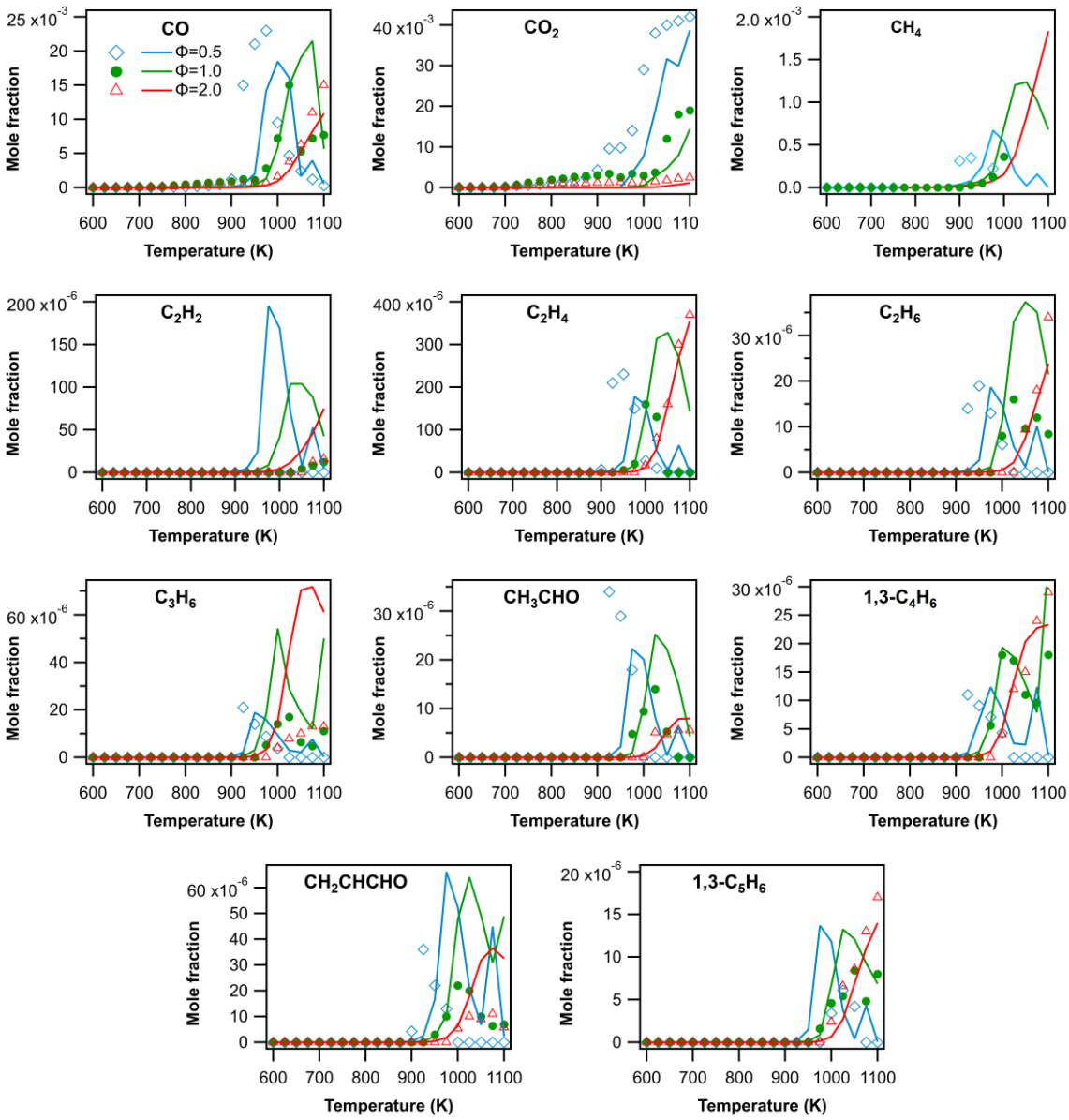

Figure S60: Experimental and simulated temperature evolution at the three equivalence ratios of non-aromatic products during p-xylene oxidation.

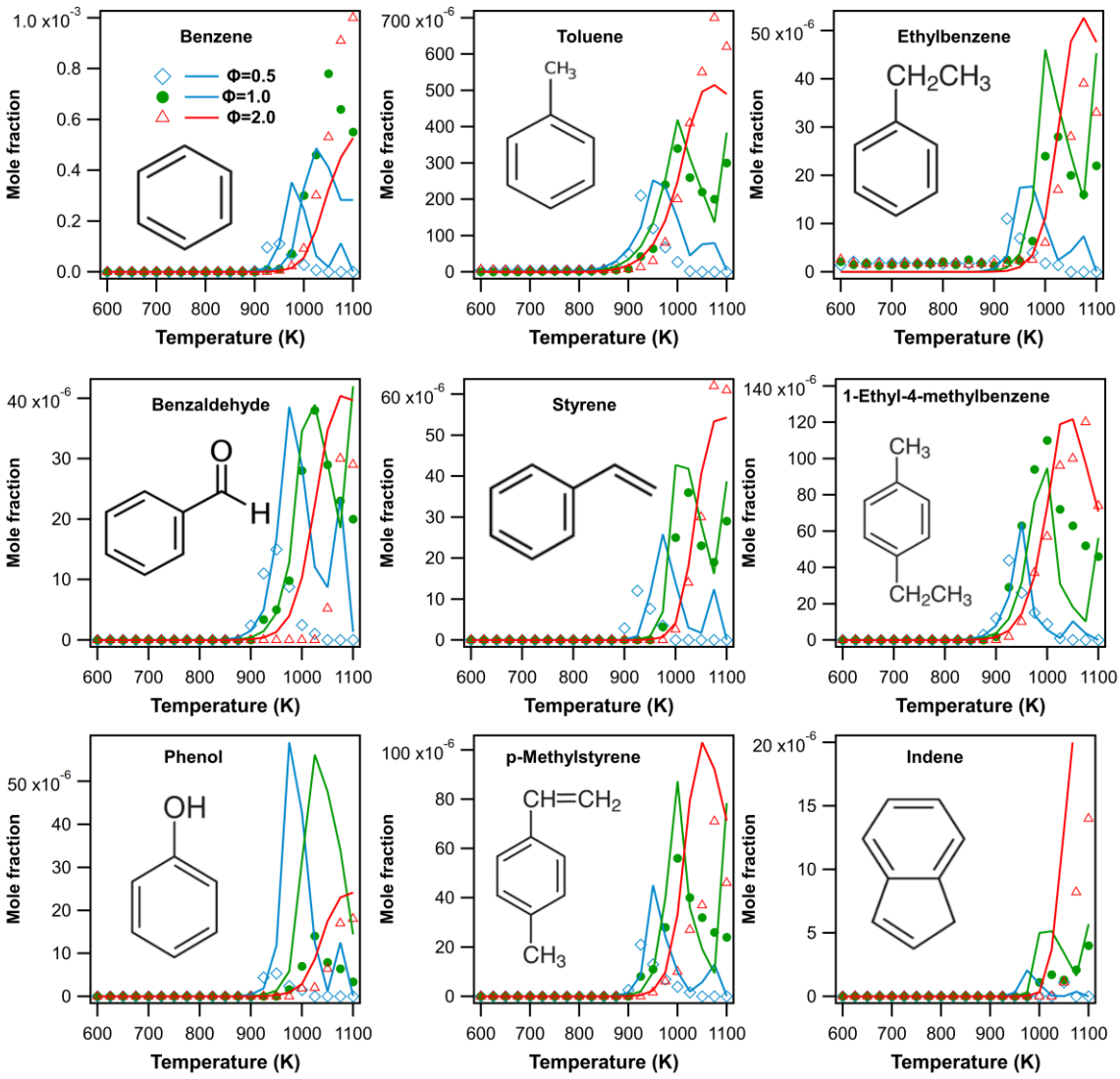

Figure S61: Experimental and simulated temperature evolution at the three equivalence ratios of aromatic products during p-xylene oxidation.

5/ Repeatability

To illustrate the repeatability observed during JSR experiments, the figure S62 shows the results of two successive experiments for the oxidation of toluene under stoichiometric conditions.

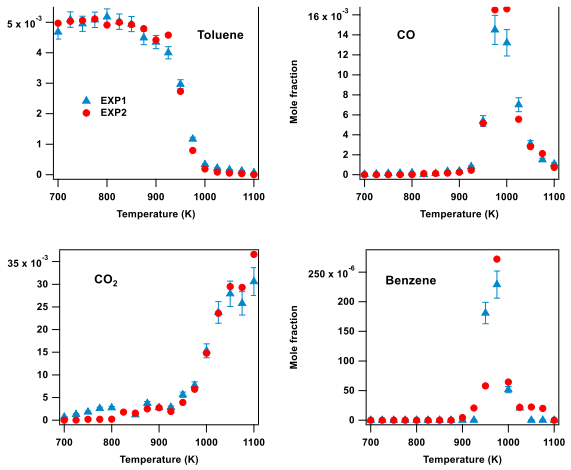

Figure S62: Results of two experiments for the oxidation of toluene (Φ=1, τ=2 s).

6/ Oscillations

To illustrate the oscillation behavior observed during JSR experiments, the figure S63 shows the numerical mole fraction of some species during the oxidation of p-xylene under stoichiometric conditions and for a temperature of 1100 K. The oscillating period is about 3.5 s.

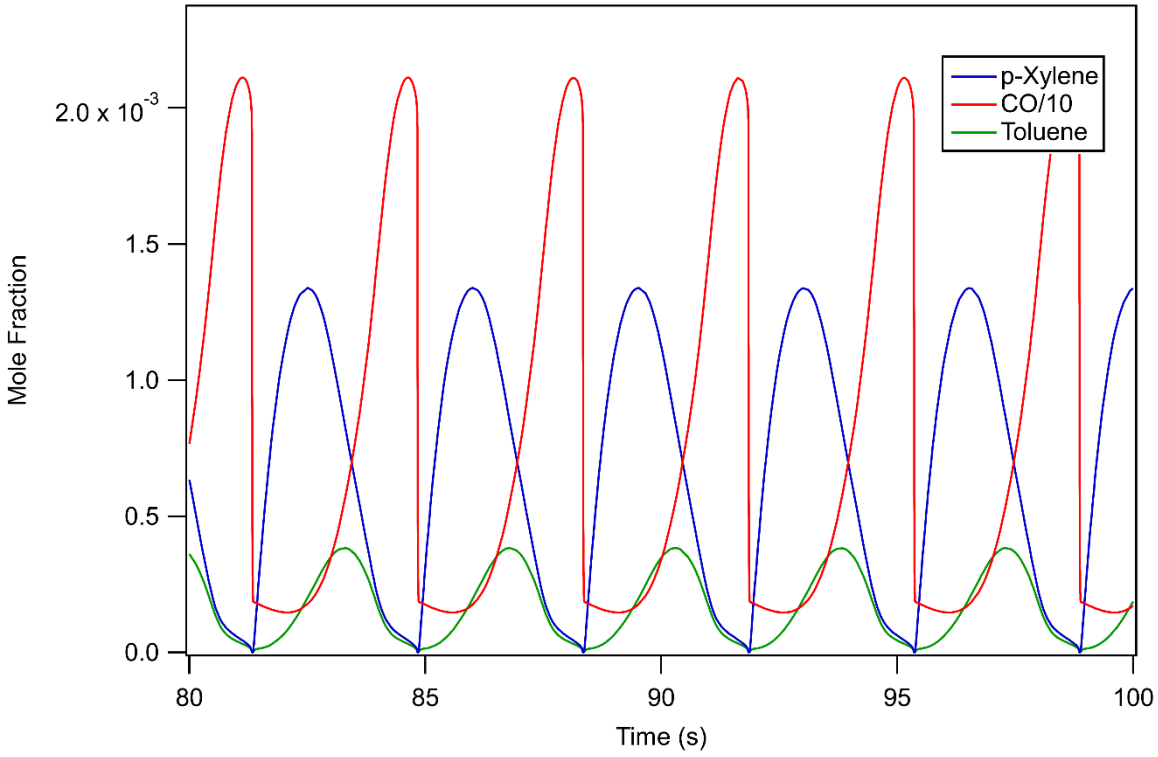

Figure S63: Oscillation behavior predicted by the COLIBRI model during the oxidation of p-xylene (Φ=1, T=1100 K, τ=2 s).

7/ Important species predicted by the model, but not detected

The following species: formaldehyde, cyclopentadienone and quinonemethide are predicted in a significant amount (~100 ppm) by the COLIBRI model but they are not detected during the experiments.

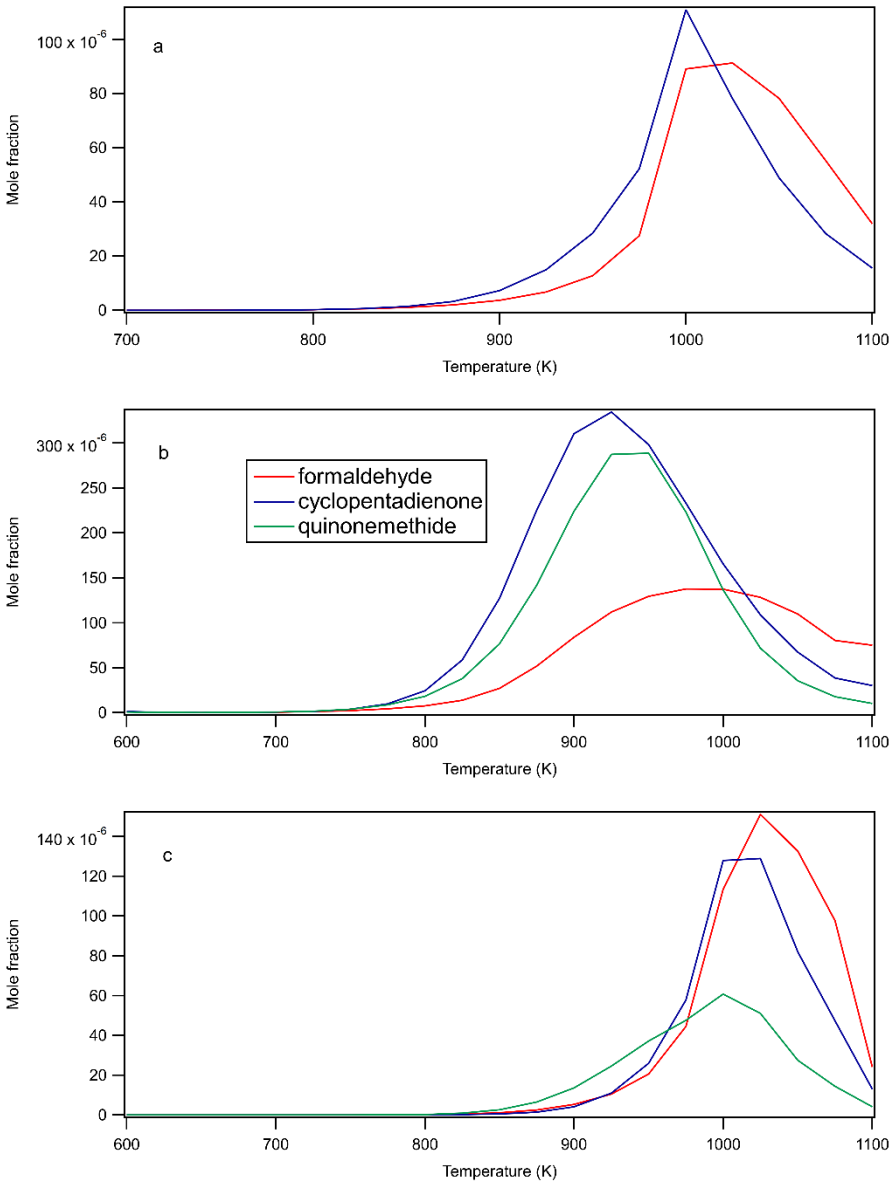

Figure S64: Numerical mole profiles of formaldehyde, cyclopentadienone and quinone methide during the oxidation of a) toluene, b) o-xylene, c) p-xylene, under stoechiometric conditions.

8/ Influence of an increased residence time

A higher residence time has been chosen compared to past studies [1,2,30–32]. Figure S65 presents a comparison between numerical species profiles obtained in JSR with a residence time of 0.1s and 2s. The longer is the residence time, the more the fuel can decompose in the reactor, that is why the fuel reactivity is shifted of 150 K between both conditions. So, it allows to study the chemistry of products at a lower temperature with the example of phenol, 2.3-dihydrobenzofuran and o-cresol. Moreover, it allows to observe new species like 1.3-benzodioxole or the low temperature behavior of phthalan around 650 K.

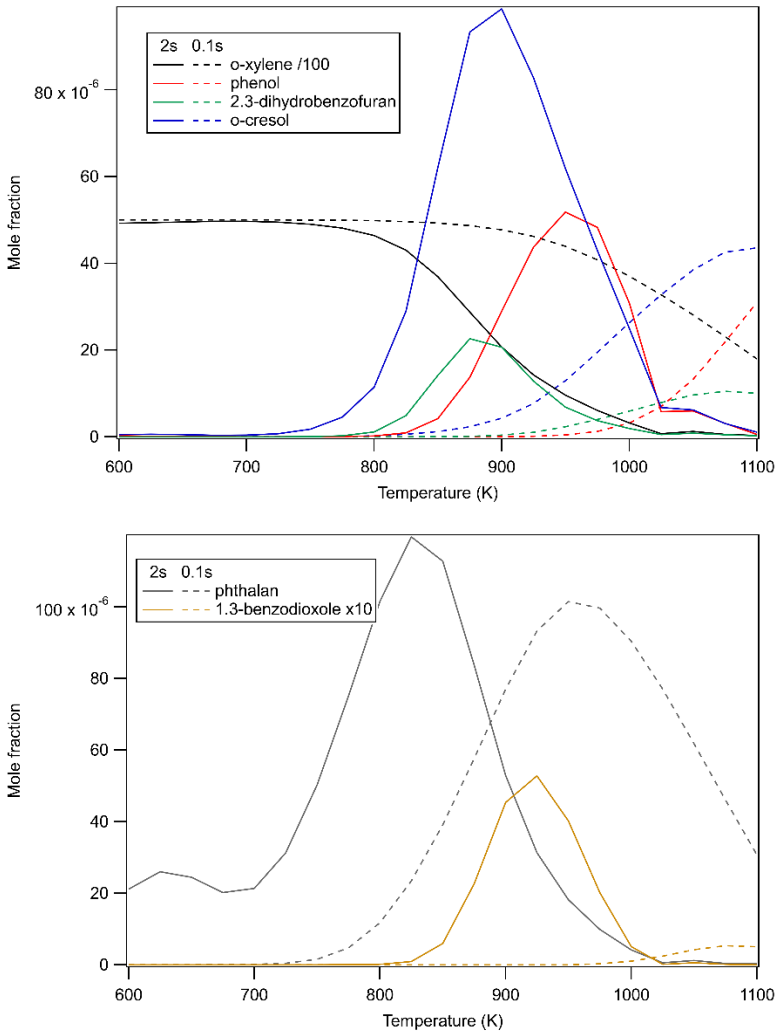

Figure S65: Comparison between numerical species profiles obtained in JSR with a residence time of 0.1s (dotted lines) and 2s (full lines).

9/ Sensitivity analysis on phthalan mole fraction

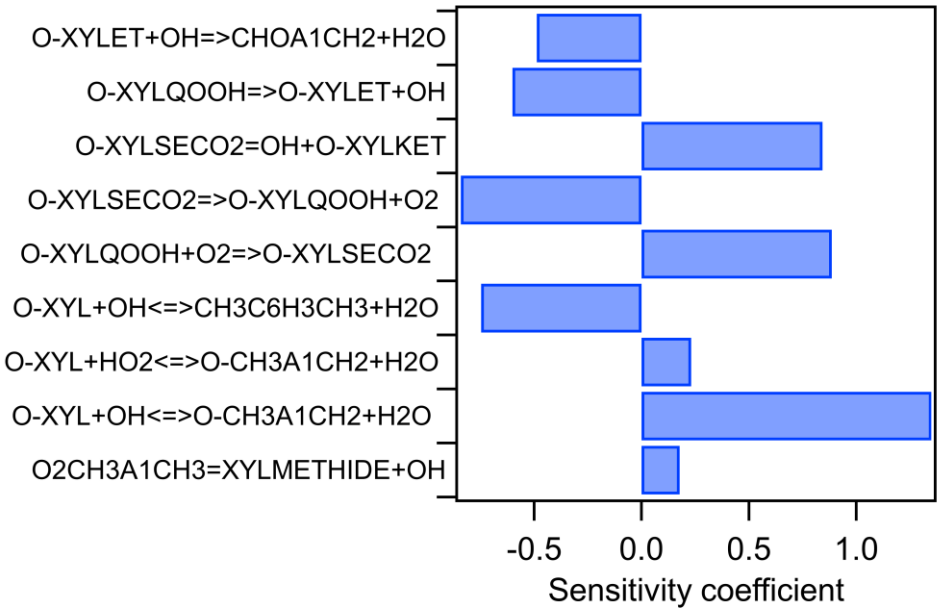

Figure S66: Sensitivity analysis on phthalan mole fraction at 650 K, same as Figure 8 of the main text but with the reactions written as in the model. Only coefficients above 0.15 are displayed.

10/ References

[1] P. Dagaut, G. Pengloan, A. Ristori, Oxidation, ignition and combustion of toluene: Experimental and detailed chemical kinetic modeling, Phys. Chem. Chem. Phys. 4 (2002) 1846–1854.

[2] W. Yuan, Y. Li, P. Dagaut, J. Yang, F. Qi, Investigation on the pyrolysis and oxidation of toluene over a wide range conditions. I. Flow reactor pyrolysis and jet stirred reactor oxidation, Combust. Flame 162 (2015) 3–21.

[3] A. Burcat, C. Snyder, T. Brabbs, Ignition Delay Times of Benzene and Toluene with Oxygen in Argon Mixtures, National Aeronautics and Space Administration, National Aeronautics and Space Administration Lewis Research Center, Cleveland, Ohio 44135, 1985.

[4] V. Vasudevan, D.F. Davidson, R.K. Hanson, Shock tube measurements of toluene ignition times and OH concentration time histories, P. Combust. Inst. 30 (2005) 1155–1163.

[5] G. Pengloan, Etude cinétique de l'oxydation de composés aromatiques: application à la formation de polluants dans les moteurs automobiles, PhD Thesis, Orléans, 2001.

[6] H.-P.S. Shen, J. Vanderover, M.A. Oehlschlaeger, A shock tube study of the auto-ignition of toluene/air mixtures at high pressures, P. Combust. Inst. 32 (2009) 165–172.

[7] G. Kukkadapu, D. Kang, S.W. Wagnon, K. Zhang, M. Mehl, M. Monge-Palacios, H. Wang, S.S. Goldsborough, C.K. Westbrook, W.J. Pitz, Kinetic modeling study of surrogate components for gasoline, jet and diesel fuels: C7-C11 methylated aromatics, P. Combust. Inst. 37 (2019) 521–529.

[8] M.B. Colket, D.J. Seery, Reaction mechanisms for toluene pyrolysis, Symp. (Int.) Combust. 25 (1994) 883–891.

[9] R. Sivaramakrishnan, R.S. Tranter, K. Brezinsky, High-pressure, high-temperature oxidation of toluene, Combust. Flame 139 (2004) 340–350.

[10] R. Sivaramakrishnan, R.S. Tranter, K. Brezinsky, High Pressure Pyrolysis of Toluene. 1. Experiments and Modeling of Toluene Decomposition, J. Phys. Chem. A. 110 (2006) 9388–9399.

[11] Y. Li, J. Cai, L. Zhang, T. Yuan, K. Zhang, F. Qi, Investigation on chemical structures of premixed toluene flames at low pressure, P. Combust. Inst. 33 (2011) 593–600.

[12] S.G. Davis, H. Wang, K. Breinsky, C.K. Law, Laminar flame speeds and oxidation kinetics of benene-air and toluene-air flames, Symp. (Int.) Combust. 26 (1996) 1025–1033.

[13] S.G. Davis, C.K. Law, Determination of and Fuel Structure Effects on Laminar Flame Speeds of C1 to C8 Hydrocarbons, Combust. Sci. Technol. 140 (1998) 427–449.

[14] T. Hirasawa, C.J. Sung, A. Joshi, Z. Yang, H. Wang, C.K. Law, Determination of laminar flame speeds using digital particle image velocimetry: Binary Fuel blends of ethylene, n-Butane, and toluene, P. Combust. Inst. 29 (2002) 1427–1434.

[15] L. Sileghem, V.A. Alekseev, J. Vancoillie, K.M. Van Geem, E.J.K. Nilsson, S. Verhelst, A.A. Konnov, Laminar burning velocity of gasoline and the gasoline surrogate components iso-octane, n-heptane and toluene, Fuel 112 (2013) 355–365.

[16] P. Dirrenberger, P.A. Glaude, R. Bounaceur, H. Le Gall, A.P. da Cruz, A.A. Konnov, F. Battin-Leclerc, Laminar burning velocity of gasolines with addition of ethanol, Fuel 115 (2014) 162–169.

[17] Y.-H. Liao, W.L. Roberts, Laminar Flame Speeds of Gasoline Surrogates Measured with the Flat Flame Method, Energ. Fuel. 30 (2016) 1317–1324.

[18] C. Ji, E. Dames, H. Wang, F.N. Egolfopoulos, Propagation and extinction of benzene and alkylated benzene flames, Combust. Flame 159 (2012) 1070–1081.

[19] D. Han, S. Deng, W. Liang, P. Zhao, F. Wu, Z. Huang, C.K. Law, Laminar flame propagation and nonpremixed stagnation ignition of toluene and xylenes, P. Combust. Inst. 36 (2017) 479–489.
[20] G. Wang, Y. Li, W. Yuan, Z. Zhou, Y. Wang, Z. Wang, Investigation on laminar burning velocities of benzene, toluene and ethylbenzene up to 20 atm, Combust. Flame 184 (2017) 312–323.
[21] K. Kumar, C.-J. Sung, Flame Propagation and Extinction Characteristics of Neat Surrogate Fuel Components, Energ. Fuel. 24 (2010) 3840–3849.
[22] C. Ji, F.N. Egolfopoulos, Flame propagation of mixtures of air with binary liquid fuel mixtures, P. Combust. Inst. 33 (2011) 955–961.
[23] X. Hui, A.K. Das, K. Kumar, C.-J. Sung, S. Dooley, F.L. Dryer, Laminar flame speeds and extinction stretch rates of selected aromatic hydrocarbons, Fuel 97 (2012) 695–702.
[24] J.D. Munzar, B. Akih-Kumgeh, B.M. Denman, A. Zia, J.M. Bergthorson, An experimental and reduced modeling study of the laminar flame speed of jet fuel surrogate components, Fuel 113 (2013) 586–597.
[25] B.-J. Zhong, H.-S. Peng, D. Zheng, The effect of different class of hydrocarbons on laminar flame speeds of three C7 fuels, Fuel 225 (2018) 225–229.
[26] Y. Zhang, Q. Li, H. Liu, Z. Yan, Z. Huang, Comparative study on the laminar flame speeds of methylcyclohexane-methanol and toluene-methanol blends at elevated temperatures - ScienceDirect, Fuel 245 (2019) 534–543.
[27] Y. Wu, B. Rossow, V. Modica, X. Yu, L. Wu, F. Grisch, Laminar flame speed of lignocellulosic biomass-derived oxygenates and blends of gasoline/oxygenates, Fuel 202 (2017) 572–582.
[28] X. Hui, C.-J. Sung, Laminar flame speeds of transportation-relevant hydrocarbons and jet fuels at elevated temperatures and pressures, Fuel 109 (2013) 191–200.
[29] R.J. Johnston, J.T. Farrell, Laminar burning velocities and Markstein lengths of aromatics at elevated temperature and pressure, P. Combust. Inst. 30 (2005) 217–224.
[30] S. Gaïl, P. Dagaut, Experimental kinetic study of the oxidation of p-xylene in a JSR and comprehensive detailed chemical kinetic modeling, Combust. Flame 141 (2005) 281–297.
[31] S. Gaïl, P. Dagaut, Oxidation of m-xylene in a JSR: experimental study and detailed chemical kinetic modeling, Combust. Sci. Technol. 179 (2007) 813–844.
[32] S. Gaïl, P. Dagaut, G. Black, J.M. Simmie, Kinetics of 1,2-Dimethylbenzene Oxidation and Ignition: Experimental and Detailed Chemical Kinetic Modeling, Combust. Sci. Technol. 180 (2008) 1748–1771.
[33] W. Yuan, L. Zhao, S. Gaïl, J. Yang, Y. Li, F. Qi, P. Dagaut, Exploring pyrolysis and oxidation chemistry of o-xylene at various pressures with special concerns on PAH formation, Combust. Flame 228 (2021) 351–363.
[34] H.-P.S. Shen, M.A. Oehlschlaeger, The autoignition of C8H10 aromatics at moderate temperatures and elevated pressures, Combust. Flame 156 (2009) 1053–1062.
[35] S. Gudiyella, T. Malewicki, A. Comandini, K. Brezinsky, High pressure study of m-xylene oxidation, Combust. Flame 158 (2011) 687–704.
[36] W. Sun, A. Hamadi, F.E.C. Ardila, S. Abid, N. Chaumeix, A. Comandini, Insights into pyrolysis kinetics of xylene isomers behind reflected shock waves, Combust. Flame 244 (2022) 112247.
[37] L. Zhao, Z. Cheng, L. Ye, F. Zhang, L. Zhang, F. Qi, Y. Li, Experimental and kinetic modeling study of premixed o-xylene flames, P. Combust. Inst. 35 (2015) 1745–1752.
[38] W. Yuan, L. Zhao, J. Yang, Z. Zhou, Y. Li, F. Qi, Insights into the Decomposition and Oxidation Chemistry of p-Xylene in Laminar Premixed Flames, J. Phys. Chem. A. 125 (2021) 3189–3197.

[39] L. Dupont, H.Q. Do, G. Capriolo, A.A. Konnov, A. El Bakali, Experimental and kinetic modeling study of para-xylene chemistry in laminar premixed flames, Fuel 239 (2019) 814–829.
[40] Y. Li, L. Zhang, Z. Tian, T. Yuan, J. Wang, B. Yang, F. Qi, Experimental Study of a Fuel-Rich Premixed Toluene Flame at Low Pressure, Energ. Fuel. 23 (2009) 1473–1485.